CONTRIBUTIONS FROM THE MUSEUM OF PALEONTOLOGY

THE UNIVERSITY OF MICHIGAN

VOL. 29, NO. 13, PP. 359-401 November 29, 1996

ANCALECETUS SIMONSI, A NEW DORUDONTINE ARCHAEOCETE (MAMMALIA, CETACEA) FROM THE EARLY LATE EOCENE OF WADI HITAN, EGYPT

BY

PHILIP D. GINGERICH AND MARK D. UHEN

MUSEUM OF PALEONTOLOGY
THE UNIVERSITY OF MICHIGAN
ANN ARBOR

CONTRIBUTIONS FROM THE MUSEUM OF PALEONTOLOGY

Philip D. Gingerich, Director

This series of contributions from the Museum of Paleontology is a medium for publication of papers based chiefly on collections in the Museum. When the number of pages issued is sufficient to make a volume, a title page and a table of contents will be sent to libraries on the mailing list, and to individuals on request. A list of the separate issues may also be obtained by request. Correspondence should be directed to the Museum of Paleontology, The University of Michigan, Ann Arbor, Michigan 48109-1079.

VOLS. 2-29. Parts of volumes may be obtained if available. Price lists are available upon inquiry.

ANCALECETUS SIMONSI, A NEW DORUDONTINE ARCHAEOCETE (MAMMALIA, CETACEA) FROM THE EARLY LATE EOCENE OF WADI HITAN, EGYPT

by

PHILIP D. GINGERICH and MARK D. UHEN

Abstract—A new advanced archaeocete, *Ancalecetus simonsi*, is described from the Birket Qarun Formation (earliest Priabonian, late Eocene) of Wadi Hitan in western Fayum Province, Egypt. *A. simonsi* is similar to *Dorudon atrox* in many ways but differs conspicuously in having fused elbows, other distinctive features of forelimb structure, and a more curved malleus within the middle ear. *Ancalecetus* appears to have been a viable if highly-specialized evolutionary experiment, an experiment that may have contributed nothing to subsequent evolution of cetaceans, but an experiment nevertheless broadening our understanding of the morphological diversity of archaeocetes.

INTRODUCTION

Wadi Hitan (Valley of Whales or Zeuglodon Valley) is a broad, flat valley in the western desert of Egypt (Fig. 1) located in Fayum Province at the western edge of the Fayum topographic depression. The geology here was first surveyed by Hugh J. L. Beadnell in the winter of 1902-1903 as part of an investigation of the suitability of the Fayum Depression for diversion and storage of Nile River water. This area was further surveyed in the winter of 1903-1904, and Charles W. Andrews (1906) described a new genus and species of archaeocete whale, *Prozeuglodon atrox* (now *Dorudon atrox*), based on the cranium and dentary of a juvenile individual from "a valley about 12 kilometers W.S.W. of the hill called Gar-el-Gehannem." This valley is Wadi Hitan, and Andrews, writing of *P. atrox* (1906, p. 244), mentioned that remains of this genus and species are found in abundance in Wadi Hitan.

Publication of monographs on or including archaeocete whales by Stromer (1903, 1908), Fraas (1904), and Andrews (1906) seemingly satisfied interest in Egyptian archaeocetes for much of the rest of the century. Henry Fairfield Osborn visited Wadi Hitan or Zeuglodon Valley briefly in 1907 (Osborn, 1907). A field party from the University of California visited Wadi Hitan for three days in 1947 (when UCMP 93169, a good cranium of *Basilosaurus isis* was collected), and Yale and Duke University field parties visited Wadi Hitan on several occasions in the 1960s through early 1980s (when YPM 24851, a nice dentary of the sirenian *Eotheroides* was collected (see Domning et al., 1982). Kellogg (1936) and Barnes and Mitchell (1978) reviewed Egyptian archaeocetes, including the few specimens then known from Wadi Hitan.

TABLE 1—Anatomical abbreviations employed in text and figures. Abbreviations of names of bones begin with a capital letter; other features are abbreviated in lower case type.

ac	acromion process	**lt**	lesser tuberosity of humerus
ang	angular process	**Lun**	lunar
app	anterior process of the periotic	**M^1_1**	molar (upper or lower)
BO	basioccipital	**Mag**	magnum
BS	basisphenoid	**mdf**	mandibular foramen
C1	cervical vertebra	**mf**	mental foramen
C^1_1	canine (upper or lower)	**mm**	manubrium of malleus
Ca1	caudal vertebra	**mpt**	medial lamina of the pterygoid
cd	mandibular condyle	**Mx**	maxilla
cfh	capitular fovea of humerus	**ncr**	nuchal crest
cm	head of malleus	**oc**	occipital condyle
cnpd	coronoid process of the dentary	**P^1_1**	premolar (upper or lower)
com	column of malleus	**Pa**	parietal
cp	coracoid process	**Pal**	palatine
crh	cranial hiatus	**papr**	paroccipital process
Cun	cuneiform	**Per**	periotic
dpc	deltopectoral crest of humerus	**pgp**	postglenoid process
eam	external auditory meatus	**Pis**	pisiform
EO	exoccipital	**ppf**	posterior palatine foramen
fec	fenestra cochleae (round window)	**ppp**	posterior process of periotic
fev	fenestra vestibuli (oval window)	**ppt**	posterior process of the tympanic
fm	foramen magnum	**Pt**	pterygoid
fo	foramen ovale	**ptsn**	pterygoid sinus
fpr	falcate process (basioccipital and exoccipital)	**R**	radius
gc	glenoid cavity of scapula	**s**	spine of the scapula
gf	glenoid fossa of squamosal	**Sc**	scapula
gt	greater tuberosity of humerus	**Sca**	scaphoid
h	head of the humerus	**SO**	supraoccipital
H	humerus	**sp**	sigmoid process of the auditory bulla
hpa	humeral process of the acromion	**Sq**	squamosal
I^1_1	incisor (upper or lower)	**ssf**	supraspinous fossa
inv	involucrum of the auditory bulla	**sym**	mandibular symphysis
isf	infraspinous fossa	**Trd**	trapezoid
J	jugal	**Tzm**	trapezium
jn	jugular notch	**U**	ulna
L1	lumbar vertebra	**Unc**	unciform
lj	lacrimal surface of jugal	**V**	vomer
lpt	lateral lamina of the pterygoid	**z**	zygomatic process of the squamosal

University of Michigan field work in Wadi Hitan was initiated in 1983 when the opportunity arose to cooperate with Elwyn Simons of Duke University and join his Duke University - Cairo Geological Museum research program in Fayum. Our initial interest was acquisition of good anatomical specimens for comparison with more primitive archaeocetes known from Pakistan, but Wadi Hitan contains such an extraordinary concentration of cetacean and sirenian specimens that we soon became interested in the diversity of marine mammals preserved in the Egyptian locality.

The specimen described here, Cairo Geological Museum [CGM] specimen 42290, was found in 1985. It was originally catalogued as University of Michigan [UM] specimen 93230, but

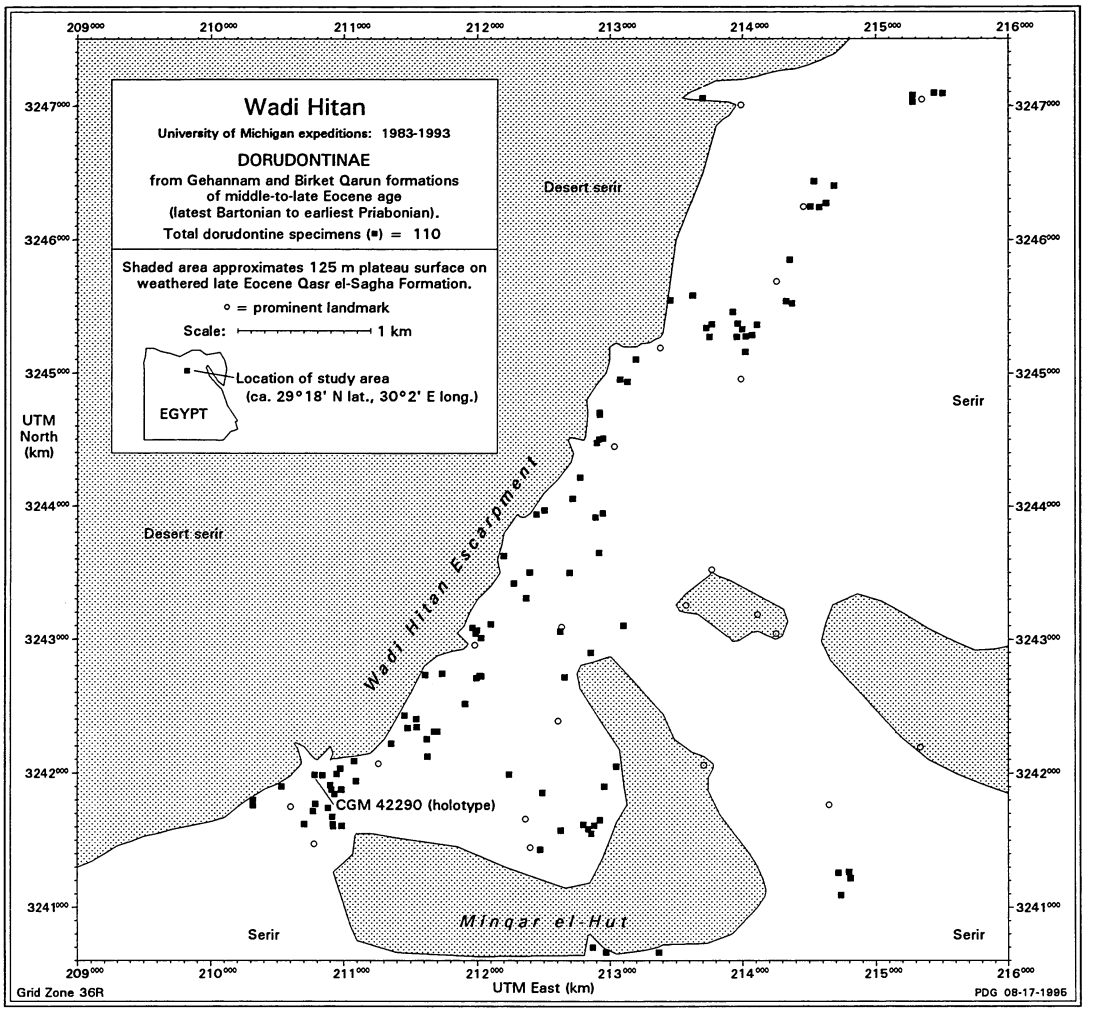

FIG. 1—Map of Wadi Hitan (Zeuglodon Valley), Egypt, showing locality of the partial skeleton of *Ancalecetus simonsi*, new genus and species, described here (CGM 42290, labeled; field designation ZV-81). Location is shown in the context of other dorundontine remains (closed squares) found in Wadi Hitan by University of Michigan expeditions. Cetaceans mapped here come from the latest Bartonian through earliest Priabonian Gehannam and Birket Qarun formations of late middle and early late Eocene age. Strata strike NE-SW and dip gently to the northwest. Shaded areas are tablelands (as shown in distance at left in Fig. 2) rising above cetacean-bearing strata and capped by indurated and erosion-resistant beds of the Umm Rigl Member of the late Eocene Qasr el-Sagha Formation. Map is 7 km × 7 km, with specimens located by reference to their positions on a triangulated field map, fit to Universal Transverse Mercator coordinates (grid zone 36R) of prominent landmarks.

renumbered when it was made a type and returned to the Cairo Geological Museum. Selected elements of CGM 42290 have been duplicated as casts and these now bear the original number UM 93230. CGM 42290 is similar to *Dorudon atrox* in many ways but differs markedly in having fused elbows and other distinctive features of forelimb structure. Description was delayed through the 1987, 1989, 1991, and 1993 field seasons because we hoped that a second specimen might be discovered. No additional remains of the fused-elbow whale have been

found, but we are now convinced that its distinctive features are not due to injury nor to pathology or developmental anomaly. The fused-elbow whale described here appears to have been a viable if highly-specialized evolutionary experiment, an experiment that may have contributed nothing to subsequent diversification of archaeocetes, but an experiment nevertheless broadening our understanding of the morphological range of archaeocetes.

ABBREVIATIONS

Institutional abbreviations used here are as follows:

CGM — Cairo Geological Museum, Cairo (Egypt)
UCMP — Museum of Paleontology, University of California, Berkeley (U.S.A.)
UM — Museum of Paleontology, University of Michigan, Ann Arbor (U.S.A.)
YPM — Yale Peabody Museum, Yale University, New Haven, Connecticut (U.S.A.)

Anatomical abbreviations are listed in Table 1.

STRATIGRAPHY AND AGE

Wadi Hitan, as noted in the introduction, is an uninhabited broad, flat, dry desert valley in a remote part of western Fayum Province in north central Egypt (Fig. 1). Bedrock strata, where exposed, are eroded continuously by wind and blowing sand. Three marine Eocene formations are exposed in Wadi Hitan. The lowest, the Gehannam Formation, is predominantly brown shale with gypsum and fine white and yellow sandstones deposited on a shallow shelf. This is Bartonian (late middle Eocene) to Priabonian (late Eocene) in age. The middle formation, the Birket Qarun Formation, is a massive yellow sandstone that is lenticular in cross-section and interpreted as an offshore barrier sandbar complex buried by a rapidly rising sea during earliest Priabonian marine transgression. The highest formation, the Qasr el-Sagha Formation, is a lagunal complex including abundant oysters and other bivalves that is Priabonian (late Eocene) in age (Gingerich, 1992).

Much of the floor of Wadi Hitan has been excavated by erosion of soft shales of the Gehannam Formation. In some areas the Gehannam Formation is overlain by indurated sandstones of the Birket Qarun Formation, while in other areas, like the type locality of the fused-elbow whale described here, the Gehannam Formation is overlain by soft sands attributed to the Birket Qarun Formation. In some areas the Gehannam Formation is overlain directly by Qasr el-Sagha Formation. Induration of bivalve-rich hard beds in the lowest Umm Rigl member of the Qasr el-Sagha Formation makes these resistant to erosion, and the Qasr el-Sagha Formation generally stands exposed as a tableland (stippled in Fig. 1) separated from eroded valleys by 20-50 m escarpments. Where the Birket Qarun Formation is thickest and most indurated, as on the southern face of Minqar el-Hut, it is eroded into spectacular sandstone cliffs standing more than 100 m above the valley floor. Much of the surface of valley floors and high tablelands is covered with a desert pavement or serir of siliceous gravel.

The ages of Wadi Hitan strata are constrained by the succession of microfossil, invertebrate, and vertebrate fossils studied in Fayum and elsewhere in northern Egypt, and by evidence of a low sea stand in Wadi Hitan itself (reviewed in Gingerich, 1992). This low sea stand corresponds to a major marine regression bringing sea level low enough to accommodate mangrove at the end of Bartonian time (end of the middle Eocene), and the Birket Qarun barrier bar complex was evidently buried by rapid sea level rise just after the low stand. These events refine correlation based on other evidence, and mean that most of the Gehannam Formation is late Bartonian, while the uppermost Gehannam, laterally equivalent Birket Qarun,

FIG. 2—Photograph of excavation of *Ancalecetus simonsi* new genus and species, CGM 42290 (holotype, ZV-81), in the context of surrounding landmarks. Desert surface here is approximately the top of the Gehannam Formation, with remnants of overlying Birket Qarun Formation represented by sandstone inselbergs in the foreground and cliffs in the left distance (on the sides of the west end of the table-like highland Minqar el-Hut shown on the map in Fig. 1). Excavation is some 2 m in diameter, just to the right of the car, in a dry wash that flooded during the winter after the specimen was collected (when remnants of plaster and burlap were buried under some 10-20 cm of waterborne sediment). View is to the south.

and overlying Qasr el-Sagha formations are Priabonian (Gingerich, 1992). Wadi Hitan is best known paleontologically for its abundant fossil cetaceans and sirenians. These come from both latest Bartonian and earliest Priabonian strata. There is no indication of significant faunal change in the Wadi Hitan stratigraphic section, and it is not possible to tell the late Bartonian and early Priabonian apart locally using macroinvertebrates or vertebrate fossils.

The type specimen of *Ancalecetus simonsi* described here, CGM 42290, is considered to be earliest Priabonian in age because it comes from the Birket Qarun Formation some 5-10 m above the base of the Minqar Abyad stratigraphic section measured in Wadi Hitan (fig. 41 in Gingerich, 1992), which places it just above the base of the Birket Qarun barrier bar complex and just above the beginning of Priabonian transgression (see also figs. 43 and 44 in Gingerich, 1992).

SYSTEMATIC PALEONTOLOGY

Order CETACEA Brisson, 1762
Suborder ARCHAEOCETI Flower, 1883
Family BASILOSAURIDAE Cope, 1868
Subfamily DORUDONTINAE (Miller, 1924)

Ancalecetus simonsi, new genus and species
Figs. 3-7, 8A, 9-22, 23A, 24-25, 27A

Holotype.—CGM 42290, including a partial cranium, left and right dentaries, vertebrae, parts of ribs, sternal elements, and much of both forelimbs.

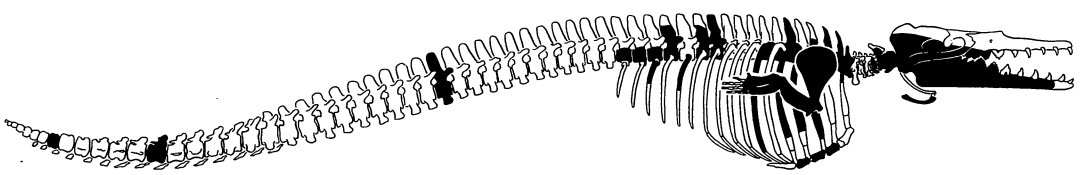

FIG. 3—Known remains (shaded) of the type and only specimen of *Ancalecetus simonsi*, CGM 42290 (holotype), superimposed on a reconstruction of the skeleton. Front and top of skull were removed by wind erosion with deflation of desert surface. Skeleton is shown in lateral view. Skull, as reconstructed, is approximately 85 cm long, and entire skeleton is approximately 5 m long.

Type locality.—Wadi Hitan locality ZV-81 (see map in Fig. 1 and photograph in Fig. 2). Stratigraphic position of the type locality in the Birket Qarun Formation is at approximately the 5-10 m level in the Minqar Abyad stratigraphic section published by Gingerich (1992, fig. 41; see discussion above).

Referred specimens.—None.

Age and distribution.—Early Priabonian, early late Eocene.

Diagnosis.—Ancalecetus simonsi differs conspicuously from all other known archaeocetes and from modern whales in having anteroposteriorly-narrow scapulae, very limited mobility of the humerus relative to the scapula at the shoulder joint, and fusion of the humerus, ulna, and radius at the elbow joint. Carpal bones of the wrist are small like those of *Zygorhiza*, but *Ancalecetus* differs from *Zygorhiza* in having the magnum-trapezoid conjoined as a single bone.

Etymology.—Ankale, Gr., bent arm, and *ketos*, whale (masc.). Species is named for Dr. Elwyn L. Simons, who discovered the type specimen in 1985, in recognition of his interest in early cetaceans and his willingness to promote this research in Egypt.

Description.—Known elements of *Ancalecetus simonsi* are shown in Figure 3. The cranium, dentaries, dentition, thyrohyal, partial vertebral column, partial rib cage, and forelimbs are described in sequence here. Abbreviations of anatomical terms are listed in Table 1. Comparative references for the osteology of archaeocetes and modern mammals include Flower (1885), Kellogg (1936), and Miller, Christensen, and Evans (1964). Measurements are in mm unless stated otherwise. The pattern for presentation of measurements is as follows: L = length; W = width; H = height. Long bones are measured as L; MLW (= mesiolateral width); and APH, DPH, or DVH (= anteroposterior, dorsoplantar, or dorsoventral height), respectively; with multiple MLW widths and APH, DPH, or DVH heights for long bones given in the sequence p : m : d = proximal : mesial : distal.

Cranium

The cranium of *Ancalecetus simonsi*, CGM 42290, is illustrated in Figures 4-6. All of the top of the skull was destroyed by erosion before the specimen was found, and nothing remains of the nasal or frontal portions of the skull. Nothing can be observed of the endocranium. However, the posteroventral part of the skull is in good condition, and preserved elements here are similar to those of *Zygorhiza* (Kellogg, 1936) and *Dorudon* (Uhen, 1996). Cranial measurements are given in Table 2.

Palate

Maxilla.—Premaxillae are not preserved, and most of both maxillae are missing as well. The only remnants of maxillae (**Mx** in Figs. 4-5) are fragmentary extensions of the palate sutured to the palatines. Posterior palatine foramina (**ppf**) that carried nerves and blood vessels supplying the palate are present in or near the maxillopalatine suture (the course of this suture is uncertain in places).

Palatine.—The palatines (**Pal** in Figs. 4-5) are paired elements forming the posterior portion of the palate, extending from the maxillae in front to the pterygoids posteriorly. The two palatines join at the midline and their ventral surface forms a keel that narrows posteriorly. This is part of the posteriormost extension of the hard palate. The palatines rise dorsally and laterally along a surface that is folded inward to form a concave surface for muscle attachment. Internal surfaces of the palatines form the ventral and lateral walls of the narial passage.

Pterygoid.—The remaining portion of the palate is formed by pterygoids (**Pt** in Figs. 4-5). These too are paired elements. They articulate anteriorly with the posterior parts of the palatines. The pterygoids meet along the midline ventrally to form ventral and lateral walls of the posteriormost extension of the narial passages. The pterygoids have several extensions and surfaces that project in different directions. One of these is continuous with the ventral palatine keel described above. Another is the lateral lamina of the pterygoid (**lpt**), which angles away from the midline posteriorly. The lateral surface of the lateral lamina forms the side of the skull and the medial surface forms the anterior portion of the lateral wall of the pterygoid sinus. Posteriorly, the lateral lamina joins the squamosal, which forms the remaining portion of the lateral wall of the pterygoid sinus. The pterygoid-squamosal suture can be traced dorsally to a point where it turns sharply anteriorly (where the squamosal meets the alisphenoid), and the pterygoid makes a short contact with the alisphenoid here. The suture can be traced anteriorly and ventrally where the pterygoid meets the posterior palatine. The pterygoid-palatine suture then angles farther anteriorly and ventrally to reach the midline.

The medial lamina of the pterygoid (**mpt**) forms the medial wall of the pterygoid sinus. The medial lamina is roughly parallel to the midline and projects out from under the lateral lamina of the pterygoid on each side. The medial lamina is nearly vertical at its anterior end, and it flares posteriorly to join the anterior border of the falcate process of the basioccipital just posterior to the basioccipital-basisphenoid suture.

The medial border of the medial lamina of the pterygoid contacts the lateral edge of the vomer, but little of this contact is preserved in CGM 42290. As stated above, the lateral and medial laminae of the pterygoid together enclose a large space known as the pterygoid sinus (**ptsn**). This sinus is confluent with the tympanic cavity posteriorly and it is open ventrally.

Vomer.—The vomer (**V** in Figs. 4-5) covers most of the ventral surface of the presphenoid, as it does in other basilosaurids, but little of it is exposed. It contacts the medial border of the medial lamina of the pterygoid.

Mesocranium

Very little of the mesocranium is preserved in CGM 42290. The frontals and frontal shield were completely destroyed by erosion, and much of each parietal has been removed by erosion as well.

Parietal.—Left and right parietals (**Pa** in Fig. 6A) make up the lateral sides of the posterior portion of the skull. Only the posterior parts of each parietal are preserved here, where they are sutured to the squamosal. The parietal-squamosal suture runs diagonally dorsally and caudally across the lateral wall of the braincase to a point where it turns sharply posteriorly and intersects the nuchal crest (**ncr**). The posterior face of the dorsal parietal is covered by the supraoccipital, but much of this contact has been destroyed by erosion.

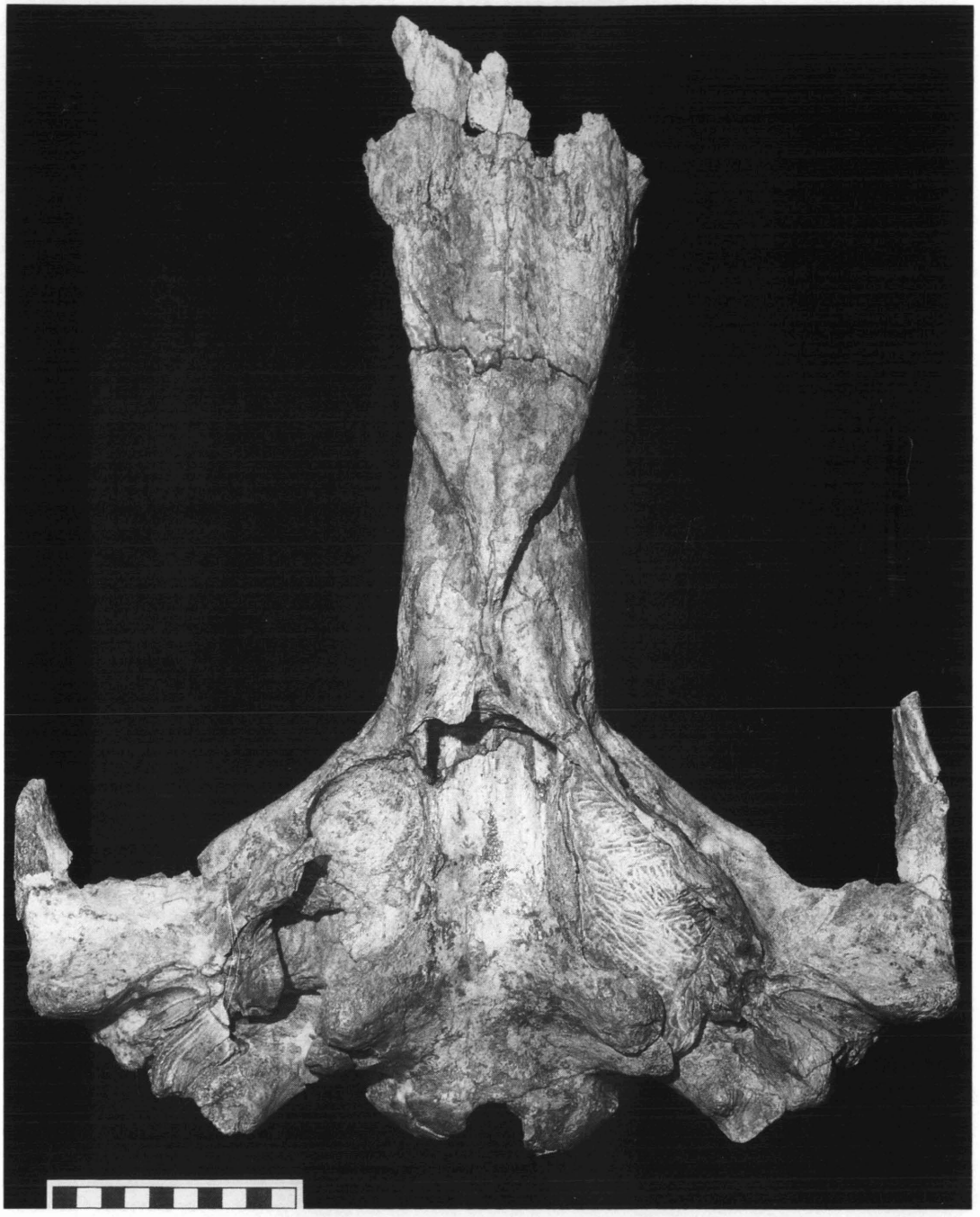

FIG. 4—Cranium of *Ancalecetus simonsi*, CGM 42290 (holotype), in ventral view. Scale is in cm. See Fig. 5 on facing page for labelling.

Abbreviations from Table 1 are: **BO**, basioccipital; **BS**, basisphenoid; **crh**, cranial hiatus; **eam**, external auditory meatus; **EO**, exoccipital; **fm**, foramen magnum; **fo**, foramen ovale; **fpr**, falcate process (of basioccipital and exoccipital); **gf**, glenoid fossa; **J**, jugal (continued on facing page ...)

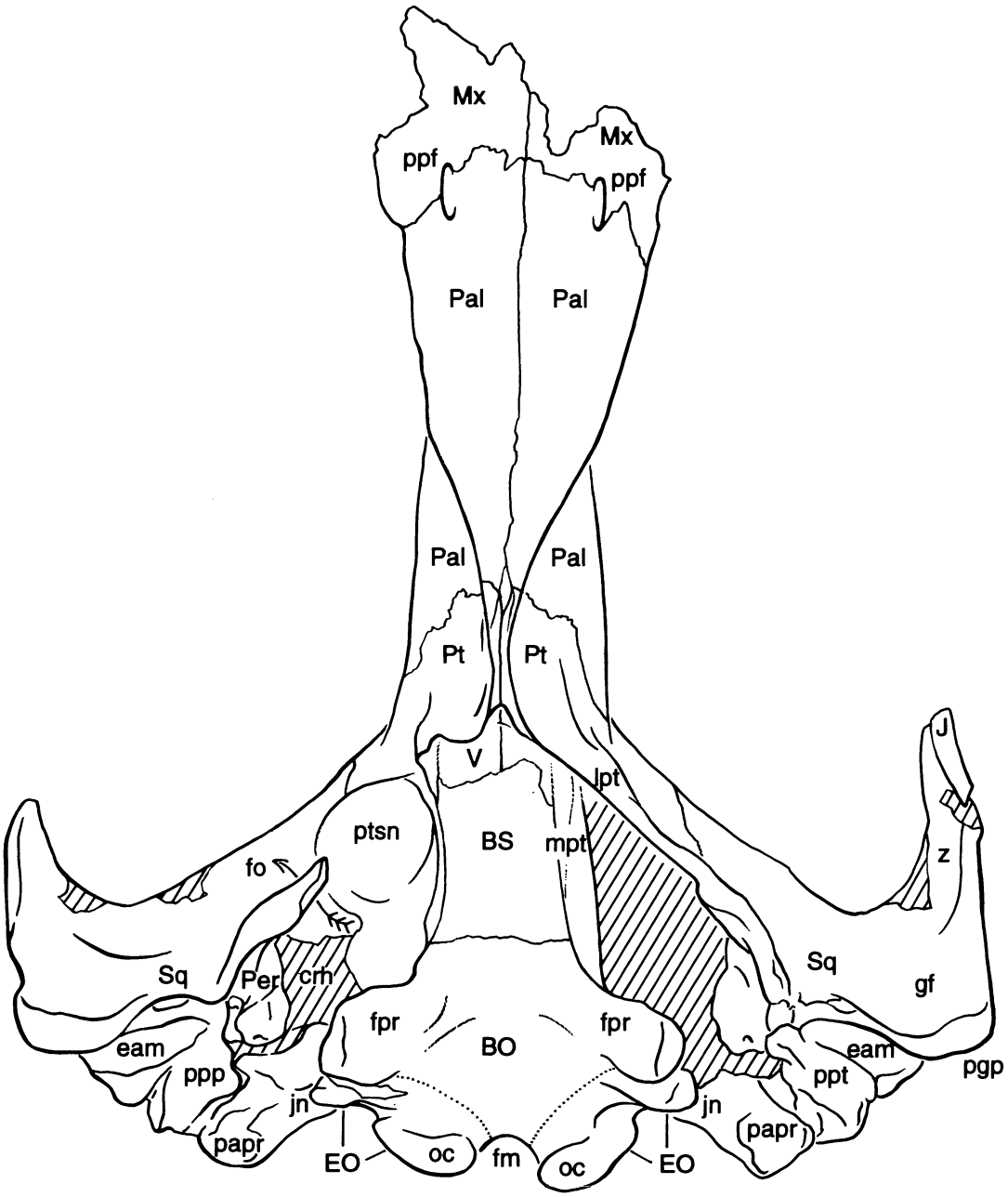

FIG. 5—Outline of cranium of *Ancalecetus simonsi*, CGM 42290 (holotype), in ventral view. Scale is given in Fig. 4.

Abbreviations continued from facing page: **jn**, jugular notch; **lpt**, lateral lamina of the pterygoid; **mpt**, medial lamina of the pterygoid; **Mx**, maxilla; **oc**, occipital condyle; **Pal**, palatine; **papr**, paroccipital process; **Per**, periotic; **pgp**, postglenoid process; **ppf**, posterior palatine foramen; **ppp**, posterior process of periotic; **ppt**, posterior process of the tympanic (attached to left *ppp*); **Pt**, pterygoid; **ptsn**, pterygoid sinus; **Sq**, squamosal; **V**, vomer; **z**, zygomatic process of the squamosal.

Orbit

All that remains of the orbital region in CGM 42290 is the ventrolateral base of each orbit in the form of left and right jugals.

Jugal.—Both jugals in CGM 42290 are preserved as isolated elements. Part of the left jugal (J in Figs. 4-5) adheres to the jugal process of the squamosal. The right jugal is the more complete (Fig. 13H). This is broadest at its anterior end where it inserted into a V-shaped notch in the maxilla. Both medial and lateral surfaces articulating with the maxilla are smooth. The dorsal surface of the jugal is triangular at the anterior end and this triangular surface (lj in Fig. 13H) is coarsely-textured where it was sutured to the lacrimal. Just posterior to this textured area, the dorsal surface curves smoothly downward and backward where it floored the orbit. Posterior to the orbit, the dorsal surface of the jugal narrows and becomes thin and bladelike where it articulated with the zygomatic process of the squamosal. The ventral surface that is V-shaped anteriorly becomes broadly rounded beneath the orbit and narrowly bladelike posterior to the orbit. The left jugal (Fig. 13G) is similar to the right jugal but lacks the anterior end; both lack posterior ends.

Basicranium

Basisphenoid.—The basisphenoid (BS in Figs. 4-5) generally has little ventral exposure on the basicranium because it is completely or almost completely covered over by vomer and pterygoids. The only portion of the basisphenoid that is visible in CGM 42290 is the ventral surface at the posterior end, where it has been exposed by breakage of the covering bones. This surface is flat and coplanar with the basioccipital. The basisphenoid-basioccipital suture is straight and runs across the basicranium perpendicular to the midline.

Alisphenoid.—The alisphenoid forms the ventral portion of the lateral wall of the mesocranium. It is discussed here as an extension of the basisphenoid. The alisphenoid covers the course of the ophthalmic and maxillary divisions of the trigeminal nerve (V_1 and V_2), beneath which is the presphenoid. Only a tiny portion of the alisphenoid is preserved in CGM 44290. A small piece of the posteroventral alisphenoid is present on each side where it contacts the palatine anteroventrally, the pterygoid posteroventrally, and the squamosal posteriorly.

Basioccipital.—The basioccipital (BO in Figs. 4-5) forms the central base of the posterior basicranium. This articulates anteriorly with the basisphenoid and posteriorly with exoccipitals. The basioccipital and exoccipitals are generally coossified in older juvenile and adult basilosaurids, but these are readily distinguished in young individuals. The caudalmost projection of the basioccipital extends between the occipital condyles and forms the ventral floor of the foramen magnum (fm). This area is also known as the intercondyloid notch. Internally, the basioccipital forms the posterior floor of the braincase.

The main body of the basioccipital is saddle-shape. Viewed ventrally, there is a broad trough along the midline formed by ventrolaterally-projecting lateral edges, which are the falcate processes (fpr) of the basioccipital. The posterior portion of each falcate process is exoccipital, and the separation of basioccipital and exoccipital is marked by a notch in the ventral edge of each falcate process.

Supraoccipital.—The supraoccipital (SO in Fig. 6B) is a singular midline bone that forms the posterior portion of the braincase and the posterior surface of the skull. Most of the supraoccipital in CGM 44290 has been weathered away, but the ventral-most portion remains. The supraoccipital articulates ventrolaterally with the exoccipitals, and the suture between these elements runs diagonally from the foramen magnum toward the ventral borders of each nuchal crest. The ventralmost projection of the supraoccipital forms the dorsal border of the foramen magnum. The posterior surface of the supraoccipital is concave, with the lateral edges flaring

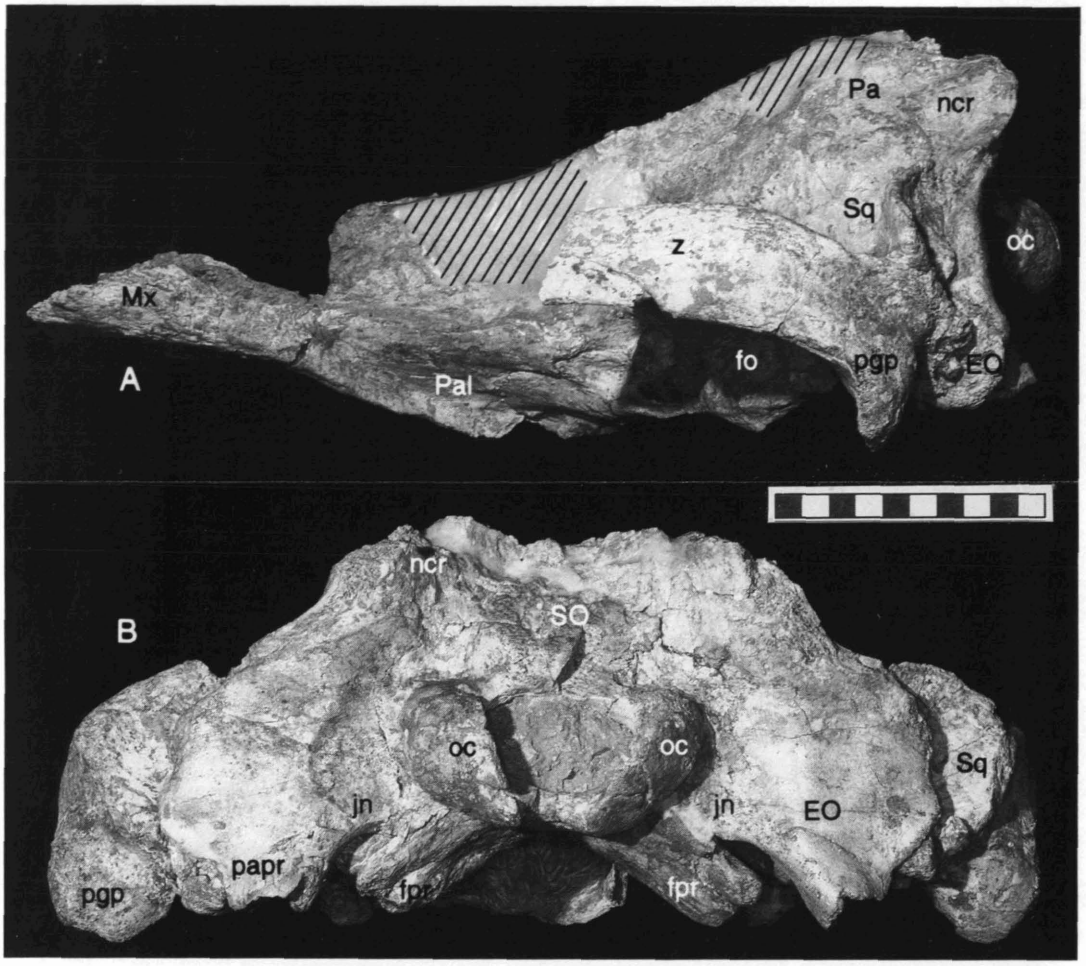

FIG. 6—Cranium of *Ancalecetus simonsi*, CGM 42290 (holotype), in (A) left lateral, and (B) posterior view. Anterior and dorsal parts of skull were exposed at the desert surface and destroyed by wind erosion. Abbreviations from Table 1 are: **EO**, exoccipital; **fo**, foramen ovale; **fpr**, falcate process; **jn**, jugular notch; **Mx**, maxilla; **ncr**, nuchal crest; **oc**, occipital condyle; **Pa**, parietal; **Pal**, palatine; **papr**, paroccipital process; **pgp**, postglenoid process; **SO**, supraoccipital; **Sq**, squamosal; **z**, zygomatic process of the squamosal. Scale is in cm.

out and back to form prominent nuchal crests. In addition, the ventral extension of the supraoccipital flares outward from the center of the bone to the edge of the foramen magnum.

Exoccipital.—The exoccipitals (**EO** in Fig. 6B) are paired bones that form the ventral part of the posterior surface of the cranium. The exoccipitals articulate dorsally with the supraoccipital along the diagonal sutures mentioned above. The anterior surface of the exoccipitals articulates medially with the parietals and laterally with the squamosals. The occipital condyles (**oc**) arise from the medial edges of the exoccipitals. They extend ventrally to the suture with the basioccipital, forming the intercondylar notch mentioned above. The occipital condyles articulate with the vertebral column. Lateral and ventral to the occipital condyles, two processes of the exoccipital form the borders of the jugular notch (**jn**), which lies between them. The more medial process is the posterior (exoccipital) portion of the falcate

TABLE 2—Selected measurements of upper and lower alveoli, diastemata, cranium, and dentary of *Ancalecetus simonsi* based on CGM 42290 (holotype). Abbreviations in the table: D, diastema following tooth; H, height; L, length; W, width. Asterisks mark estimated measurements; superscript *a* indicates an estimate is of the length or width of an alveolus (alveoli in the case of teeth with multiple roots). Measurements are in blocks of mm and cm, as noted.

Cranium									
I^1	L:W:H:D:	–	:	–	:	–	:	–	mm
I^2	L:W:H:D:	–	:	–	:	–	:	–	
I^3	L:W:H:D:	–	:	–	:	–	:	–	
C^1	L:W:H:D:	–	:	–	:	–	:	–	
P^1	L:W:H:D:	–	:	–	:	–	:	–	
P^2	L:W:H:D:	–	:	–	:	–	:	–	
P^3	L:W:H:D (double-rooted):	61.4	:	20.8	:	47.0*	:	–	
P^4	L:W:H:D (double-rooted w. medial buttress):	46.6	:	22.6	:	35.0*	:	0.0	
M^1	L:W:H:D (double-rooted):	29.0*	:	16.5*	:	–	:	–	
M^2	L:W:H:D:	–	:	–	:	–	:	–	
	Skull length (condylobasal):							–	cm
	Diameter of orbit:							–	
	Diameter of infraorbital foramen:							–	
	Breadth of frontal shield at postorbital process (maximum):							–	
	Breadth across nasals on frontal shield (maximum):							–	
	Breadth of rostrum at C^1:							–	
	Breadth of rostrum at P^2:							–	
	Breadth of palate at M^3:							–	
	Height of skull above palate at M^{2-3}:							–	
	Breadth of skull across zygomatic arches (maximum):							–	
	Breadth of skull across squamosals:							39.0	
	Breadth of skull across exoccipitals:							28.0	
	Foramen magnum W:H:					5.6	:	3.5	
	Height of nuchal crest above foramen magnum (maximum):							–	
	Tympanic bulla L:W:H:			8.2	:	5.5	:	5.1	
Mandible									
I_1	L:W:H:D:	–	:	–	:	–	:	–	mm
I_2	L:W:H:D:	–	:	–	:	–	:	–	
I_3	L:W:H:D:(single-rooted alveolus):	–	:	–	:	–	:	19.4	
C_1	L:W:H:D (single-rooted alveolus):	–	:	–	:	–	:	29.5	
P_1	L:W:H:D (double-rooted, confluent roots):	35.8	:	18.5	:	–	:	13.7	
P_2	L:W:H:D (double-rooted):	53.1	:	20.1	:	–	:	10.5	
P_3	L:W:H:D (double-rooted):	65.3	:	24.0	:	–	:	0.0	
P_4	L:W:H:D (double-rooted):	58.9	:	20.4*	:	–	:	0.0	
M_1	L:W:H:D (double-rooted):	37.1	:	18.3	:	–	:	0.0	
M_2	L:W:H:D (double-rooted):	35.4	:	19.1	:	–	:	0.0	
M_3	L:W:H (double-rooted):	34.7	:	17.5	:	–	:		
	Length of left dentary from front of C_1 alveolus to back of M_3 alveolus:							41.5	cm
	Depth of dentary below C_1:							5.5	
	Depth of dentary below P_{3-4}:							8.3	
	Depth of dentary below M_1:							9.7	
	Depth of dentary below M_3:							13.5	
	Posterior opening of mandibular canal W:H:					4.5	:	10.4	

process (**fpr**) described above because it joins part of the basioccipital. The more lateral process is the paroccipital process (**papr**). Just lateral to the paroccipital process is a posterior flare of the exoccipital that forms a small arch of bone. Lateral portions of the exoccipital form the posterior surface of the skull. These are broadly scalloped and do not extend as far laterally as the squamosals, leaving the posterior surfaces of left and right squamosals partially exposed.

Squamosal.—The squamosal (**Sq** in Figs. 4-6) forms the posterolateral wall of the side of the cranium. The squamosal articulates anteriorly along its dorsal edge with the parietal and on its anteroventral edge meets the alisphenoid as described above. There is also a contact with the pterygoid, enclosing the foramen ovale (**fo** in Figs. 4-5 and 6A) that carried the mandibular branch of the trigeminal nerve (V_3) into the temporal fossa. On the ventral side, the squamosal has a complex relationship with the periotic (described below). The posterior surface of the squamosal is sutured to the anterior face of the exoccipital. Together these bones form the lateral portion of the nuchal crest. The suture between the squamosal and exoccipital lies in a groove between these bones that extends up the middle of the nuchal crest. The nuchal crest and this suture continue medially and then turn abruptly dorsally where the squamosal meets the parietal. The squamosal-parietal suture can be traced anteriorly across the anterolateral face of the nuchal crest and it then turns ventrally to meet the alisphenoid. The anterior end of the squamosal-parietal suture is visible on the sides of the skull in CGM 44290, but the posterior portion of the suture, with much of the nuchal crest, has been destroyed by weathering. The anterolateral surface of the squamosal bulges outward laterally to accommodate the parietal lobe of the brain on the internal side.

The squamosal projects laterally from the side of the skull and anteriorly to form the zygomatic process of the squamosal (**z**). Once this zygomatic process turns anteriorly it becomes laterally compressed and parallels the dorsal surface of the jugal. The two bones evidently remained separate along their entire parallel course.

The glenoid fossa (**gf**) is the articular surface for the dentary. A large postglenoid process (**pgp**) is present extending ventrally from the zygomatic process, which limits backward movement of the mandibular condyle. There is no postglenoid foramen and venous drainage from the brain is entirely through though the jugular and other veins passing out of the cranial cavity via the cranial hiatus.

Periotic.—The periotic (**Per** in Fig. 7) is an unusually dense bone, the central body or petrous part of which surrounds the inner ear. This is present on both sides but well preserved only on the right side. The anterior process of the periotic (**app**) extends anteriorly and slightly ventrally from the body. It is a broad plate of bone that comes to a rounded apex. There is a prominent posterior process (**ppp**) projecting posteriorly and laterally that is wedged between the external auditory meatus (**eam**) and squamosal in front and the exoccipital in back. The ventral surface of this posterior process articulates with a corresponding posterior process of the tympanic (**ppt**, present on the left side attached to the posterior process of the periotic). Its ventral surface is covered with a series of fine tongue and groove structures that run parallel to the long axis of the process. These tongue and groove structures of varying depth match similar structures on the dorsal surface of the posterior process of the tympanic. A third process is the superior process of the periotic, which is covered by other bones on both the left and right sides in CGM 42290.

The body of the periotic contains the inner ear and all foramina of the periotic. It is convex ventrally, forming a broad ventral promontorium. There is a lateral eminence that is the pars cochlearis of the periotic. Lateral to this lateral eminence is a groove running roughly anteroposteriorly, anterior to the fenestra vestibuli (**fev**) or oval window and medial to the fossa for the head of the malleus. Kellogg (1936) identified this groove as the place of origin of the tensor tympani muscle in *Zygorhiza kochii*. The body has some additional accessory structures associated with it. The largest of these is the fossa for the head of the malleus, located on the lateral side of the body. This is an almost circular concavity that faces ventrally and slightly

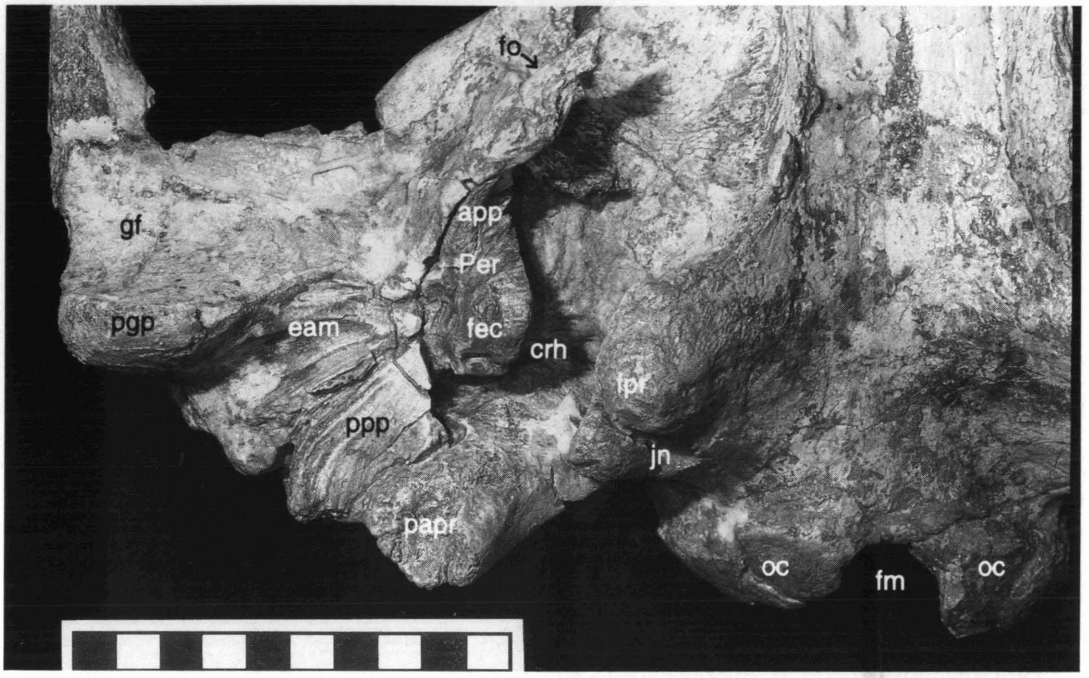

FIG. 7—Right temporal region of *Ancalecetus simonsi*, CGM 42290 (holotype), in ventral view. Abbreviations from Table 1 are: **app**, anterior process of the periotic; **crh**, cranial hiatus; **eam**, external auditory meatus; **fec**, fenestra cochleae (round window); **fev**, fenestra vestibuli (oval window, visible but not labeled); **fm**, foramen magnum; **fo**, foramen ovale; **fpr**, falcate process; **gf**, glenoid fossa; **jn**, jugular notch; **oc**, occipital condyle; **papr**, paroccipital process; **Per**, periotic; **pgp**, postglenoid process; **ppp**, posterior process of periotic. Scale is in cm.

posteriorly. It projects from the main portion of the periotic body just anterior to the fenestra vestibuli. The fenestra vestibuli or oval window is present on the lateral side of the body of the periotic. This accommodates the footplate of the stapes and opens into the vestibule of the inner ear, which communicates with the basal turn of the cochlea. The fenestra cochleae (**fec**) or round window is located on the posteroventral face of the body of the periotic. This was covered in life by a secondary tympanic membrane, equalizing pressure between the inner and middle ears. The lateral face of the body of the periotic also contains the lateral opening of the canal for the facial nerve. The internal auditory meatus is the most prominent structure on the medial (endocranial) side of the periotic in *Ancalecetus*, as in other mammals, but this is not visible in CGM 42290.

Rommel (1990) showed a foramen lacerum anterior to be located between the basisphenoid and presphenoid in *Tursiops*, but no foramen could be located in this position in *A. simonsi*, which is not surprising since the position of the brain relative to the basisphenoid-presphenoid suture is very different in archaeocetes compared to odontocetes. The foramen lacerum medium also appears to be absent. This carries the internal carotid artery into the braincase in modern cetaceans (Rommel, 1990), but it is possible that the carotid artery travels through the cranial hiatus rather than having a separate foramen. A foramen lacerum posterius is ill defined in basilosaurid cetaceans and the large fissure in its place has been called the cranial hiatus (**crh**) in modern cetaceans (Rommel, 1990). The cranial hiatus takes the form of a large fissure between the basioccipital medially and the periotic laterally. The anterior border of the cranial hiatus is formed by the squamosal, while the posterior border is formed by the exoccipi-

tal. Thus, the cranial hiatus extends from the posterior edge of the pterygoid sinus (at the posterior border of the basicranial surface of the squamosal) to the posterior edge of the basicranium at the jugular notch of the exoccipital. In life the cranial hiatus was partially covered by the auditory bulla.

Ectotympanic.—The tympanic (ectotympanic) auditory bulla of *Ancalecetus simonsi* (Fig. 13F) is a large ovate structure like that of other advanced archaeocetes (Kellogg, 1936), including *Zygorhiza kochii* (Lancaster, 1990) and *Dorudon atrox* (Uhen, 1996). It is composed of unusually dense compact bone. The left bulla is well preserved in CGM 42290 (measurements are given in Table 2). It has a convex ventral surface and a deeply excavated dorsal surface (tympanic cavity). The tympanic cavity is an anteroposteriorly elongated space opening into the middle ear above. The tympanic cavity is widest anteriorly and narrows posteriorly. There is a shallow depression on the posteroventral part of the external surface of the bulla that separates the involucrum (**inv** in Fig. 13F) on the medial side from the outer lip. The latter bears a raised circular eminence curving smoothly into the sigmoid process (**sp**). The sigmoid process curves posteriorly where it rises as a distinct process and normally would project dorsally above the rest of the bulla, however most of the sigmoid process is broken and missing. The posterior edge of the sigmoid process normally curls backward, enclosing a space between itself and the body of the auditory bulla, and a natural cast of this space is preserved in CGM 42290. Much of the malleus is present, attached to the gracile or gonial process. There is a distinct sulcus for the chorda tympani anterior to the gracile process. The posterior pedicle and the conical process are both broken and missing in CGM 42290, as is the posterior process of the tympanic (**ppt** in Figs. 4-5) by which it articulated with the posterior process of the periotic.

Malleus.—Much of the left malleus is present, firmly attached to the gracile process of the tympanic bulla (Fig. 8). There is just a trace of a suture but the two bones appear to be solidly fused. The dorsal surface of the head (**cm**) that articulated with the petrosal is missing, as are both surfaces for articulation with the incus. The column (**com**) and manubrium (**mm**) are well preserved. The column is a little longer relative to the head than in *Dorudon atrox* (UM 101222; Uhen, 1996), and the manubrium is more extended and consequently more pointed. However, the greatest difference is one of curvature. The column and manubrium of the malleus in *Ancalecetus simonsi* curve downward, medially, and anteriorly into the tympanic cavity of the bulla. This contrasts with a straighter and more horizontally-medial orientation of the column and manubrium in *Saghacetus osiris* (Pompeckj, 1922), *Zygorhiza kochii* (Lancaster, 1990, fig. 3B), and *Dorudon atrox* (Uhen, 1996). The malleus in CGM 42290 is approximately the size of that of *D. atrox*, but it has not been measured because it has not been removed from the bulla.

Mandible

Dentary.—Left and right mandibles in *Ancalecetus simonsi* are each composed of a single bone, the dentary (Figs. 9-11). In CGM 42290 the left dentary is complete from the alveolus for I_3 to the mandibular condyle (**cd**), and the right dentary is complete from the alveolus for P_1 to the mandibular condyle. The mandibular symphysis (**sym**) between these extends posteriorly to a point below the posterior edges of the alveoli for P_2. This symphysis is unfused. Rami of left and right dentaries parallel each other along the symphysis and then diverge posteriorly as far as the end of the molar series. Posterior to the molar series the rami are again more parallel. Much of the medial surface of the dentary is gently concave, while the lateral surface is slightly convex. The lateral surface bears a series of small mental foramina (**mf**). At the anterior end of the dentary these are close to the ventral border of the ramus, but successive foramina are higher on the ramus so that the last, just below the anterior root of M_1, is very near the dorsal border of the ramus. There are some seven or eight mental

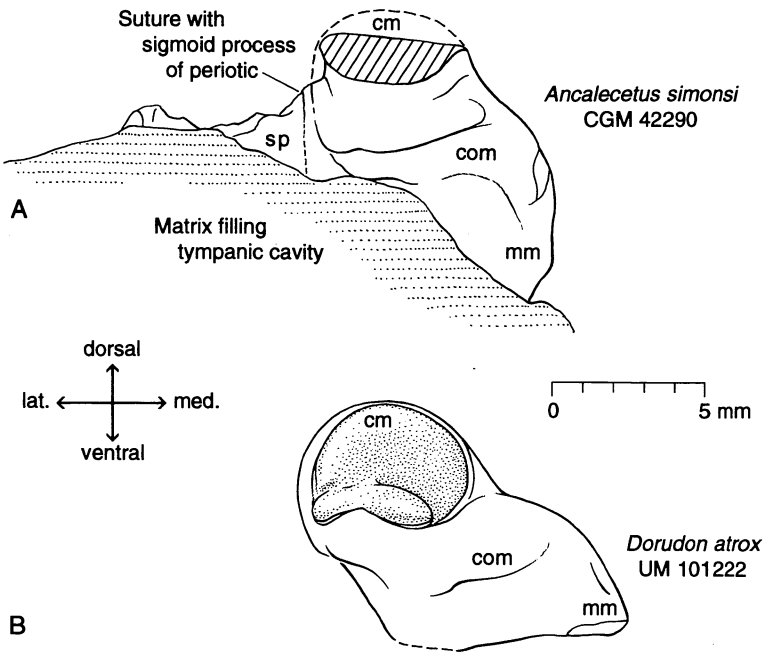

FIG. 8—Malleus of *Ancalecetus simonsi* compared to that of *Dorudon atrox*. A, malleus of *A. simonsi*, CGM 42290 (holotype), in position within the tympanic bulla; B, freestanding malleus of *D. atrox*, UM 101222). Both are shown in posterior view. Malleus of *A. simonsi* lacks part of head. Abbreviations from Table 1 are: **cm**, head of malleus; **com**, column of malleus; **mm**, manubrium of malleus. Ossified surfaces for articulation with the incus (stippled) are preserved in UM 101222 but not in CGM 42290. Note the distinctly downturned column and manubrium of the malleus in *A. simonsi*, which differs from the straighter and more medially directed column and manubrium of *Dorudon* shown here, *Saghacetus* (Pompeckj, 1922), and *Zygorhiza* (Lancaster, 1990).

foramina in total. These transmit fibers of the mandibular branch of the mandibular branch of the trigeminal nerve and also supply blood to the lower lip.

The horizontal ramus of the dentary is shallow in depth from the front to the end of the premolar series. The dentary then increases in depth as the dorsal surface of the dentary sweeps upward toward the apex of the coronoid process (**cnpd**). Lower molars are rooted in this ascending portion. The angular process (**ang**), where the lateral surface of the dentary is inflected to form the floor of the mandibular foramen, is well preserved on both sides. The mandibular foramen (**mdf**) and its extension within the dentary as a mandibular canal are both large and exceptionally well preserved in *Ancalecetus simonsi*. The lateral wall of the dentary is uniformly about 4 mm thick over an oval area of the acoustic window posterior to the mandibular foramen (Norris, 1980). The mandibular canal houses a large fat pad in modern whales that is believed to play a role in sound transmission to the middle ear. Measurements of the dentary and mandibular foramen are given in Table 2.

Dentition

The dental formula of *Ancalecetus simonsi* is almost certainly 3.1.4.2/3.1.4.3, with M^3 having been lost, as in *Dorudon atrox* and other advanced archaeocetes. Neither maxilla is

FIG. 9—Left and right dentaries of *Ancalecetus simonsi*, CGM 42290 (holotype), in occlusal view. Anterior portions of both dentaries are damaged. Scale is in cm. Note extension of the mandibular symphysis (**sym**) posteriorly as far as the posterior margin of P_2, and inflected angular process of left and right dentaries (**ang**) below and anteromedial to the mandibular condyles (**cd**).

preserved adequately to show whether M^3 was present or not, but the absence of lateral wear on M_3 makes loss of M^3 likely.

A single anterior tooth (not figured) is preserved in CGM 42290. It is difficult to determine which tooth this is because anterior teeth are generally very similar in archaeocetes. The tooth has a bulbous root, but the crown is damaged making it impossible to determine whether it is an upper or lower tooth, or whether it is from the left or right side. By chance alone it is probably a lower tooth, since the entire anterior portion of the cranium was destroyed by wind erosion.

Upper dentition.—Most of the upper dentition was destroyed by erosion. What remains is shown in Figure 13A-D. The upper premolars are represented by left and right P^{3-4}. These are double-rooted with a crown that is roughly triangular in lateral view. Posterior roots of P^4 each have a strong lingual projection that is covered by a lingual extension of the crown, but this does not appear to be the case on the one reasonably complete crown of P^3. Premolars P^{3-4} have a strongly developed central cusp, and the anterior and posterior edges of the crown are lined with accessory cusps. Anterior accessory cusps are conspicuously smaller than posterior accessory cusps. These teeth are both worn in life and damaged by erosion, making counts of cusps and precise measurements impossible.

The only upper molar preserved is right M^1. This tooth is heavily worn on the lingual side. It has two roots, with the posterior root being slightly more expanded lingually than the anterior root. The central cusp and all accessory cusps were removed by masticatory wear during life.

Lower dentition.—CGM 42290 preserves the root of a single-rooted I_3 and the alveolus for a single-rooted C_1 on the left side. Roots of P_{1-2} are preserved on the left side, and both of these teeth appear to have been double-rooted (roots of P_1 are confluent). The third lower premolar has some of the crown preserved in both dentaries, and the fourth lower premolar is well-preserved on both sides. Both P_3 and P_4 are roughly triangular in lateral view, with a

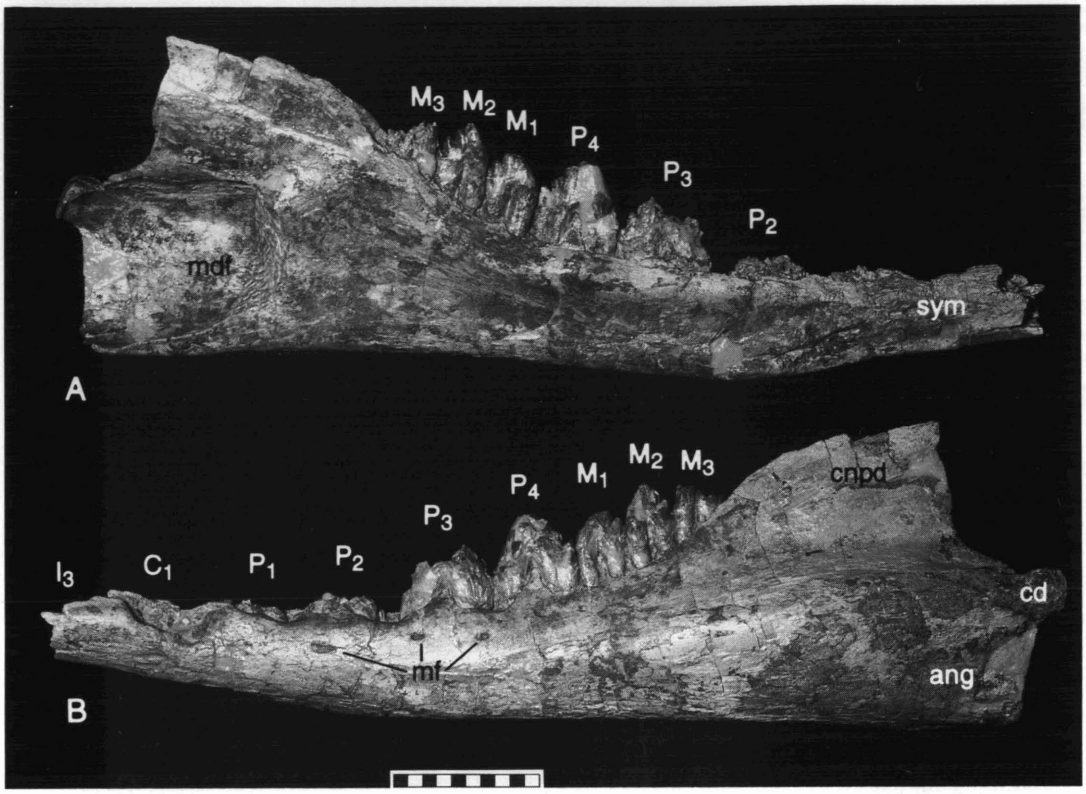

FIG. 10—Left dentary of *Ancalecetus simonsi*, CGM 42290 (holotype) in medial (A) and lateral view (B). Abbreviations from Table 1 are: **ang**, angular process; **cd**, mandibular condyle; **cnpd**, coronoid process of the dentary; **mdf**, mandibular foramen; **mf**, mental foramen; **sym**, mandibular symphysis. Scale is in cm. Note large mandibular foramen (*mdf*) leading to a large mandibular canal like that found in other advanced archaeocetes and later whales.

strong central cusp. There are accessory cusps along the anterior and posterior edges of the teeth, with again anterior cusps being smaller than posterior cusps. P_3 is a little larger than P_4 (measurements are given in Table 2).

Tooth wear.—Two modes of wear are evident on posterior premolars and molars of *Ancalecetus simonsi*. The apical and accessory cusps show evidence of wear on their tips. Figure 12 shows that the apical cusp and anterior accessory cusps closest to the apical cusp have been worn off on P_4. In addition the apical cusp of M_1 is worn off, and the apical cusp of M_2 is heavily worn. This type of wear is almost certainly due to tooth-on-food contact since it is so rounded. Tooth-on-tooth wear is evident in the lateral wear facets shown in Figure 12. There are areas where enamel is worn off of the lateral faces of the lower teeth in well-defined grooves produced when medial sides of the upper teeth sheared past lateral sides of the lower teeth. This grooved wear is patterned so that grooves correspond to individual cusps on lower molars. There are no wear facets evident on the talonid of M_3 because there was evidently no corresponding M^3.

Heavy tooth wear in *Ancalecetus simonsi* is significant in showing that the type individual fed as a normal basilosaurid, feeding on prey (presumably fish) that were large enough to re-

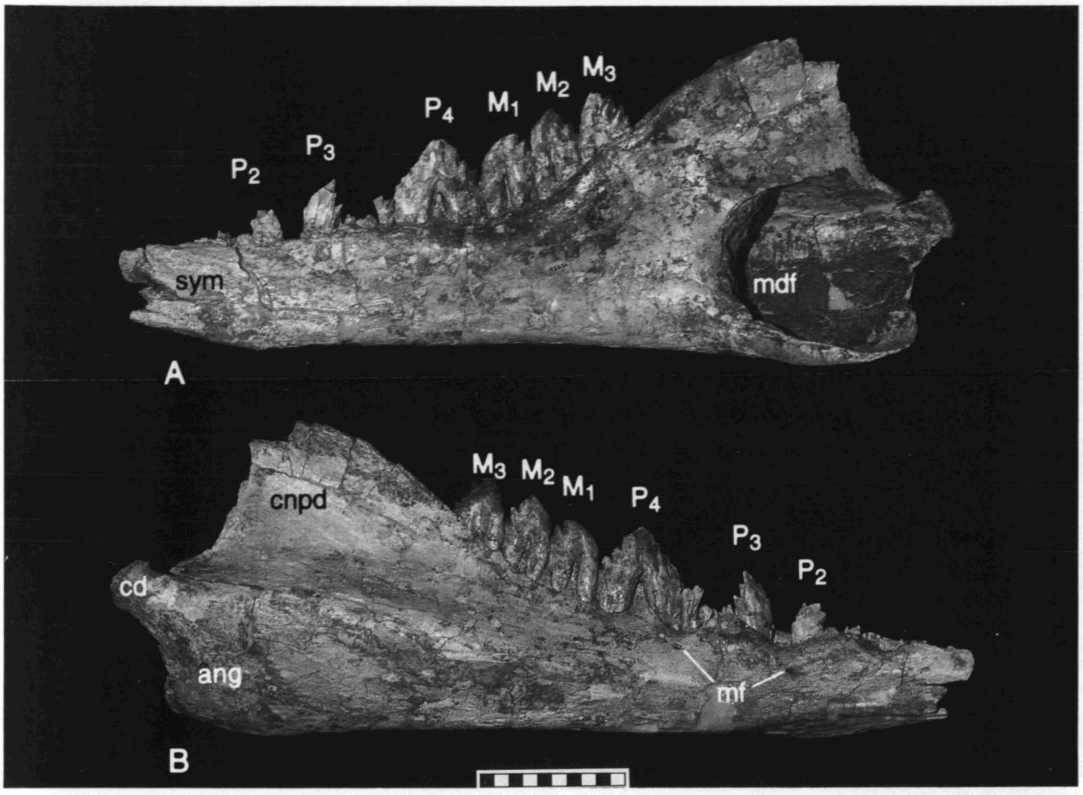

FIG. 11—Right dentary of *Ancalecetus simonsi*, CGM 42290 (holotype) in medial (A) and lateral view (B). Abbreviations from Table 1 are: **ang**, angular process; **cd**, mandibular condyle; **cnpd**, coronoid process of the dentary; **mdf**, mandibular foramen; **mf**, mental foramen; **sym**, mandibular symphysis. Scale is in cm. Note large mandibular foramen (*mdf*) leading to a large mandibular canal like that found in other advanced archaeocetes and later whales.

quire reduction through mastication before swallowing. Heavy tooth wear is also significant in showing that the type specimen was an individual that survived to adulthood.

Hyoides

Thyrohyal.—The only element of the hyoid apparatus preserved in CGM 42290 is the right thyrohyal (Fig. 13E). The thyrohyal is robust and greatly expanded on its proximal end where it was connected to the basihyal. The body is roughly triangular in cross section near the proximal articular surface but flattens and then expands slightly toward the distal end. The distal end of the thyrohyal is broken, so its morphology remains unknown.

Vertebral column

Twenty vertebrae of CGM 42290 are sufficiently well preserved to be measured and described. Measurements are given in Table 3. A length-of-vertebrae profile is shown in

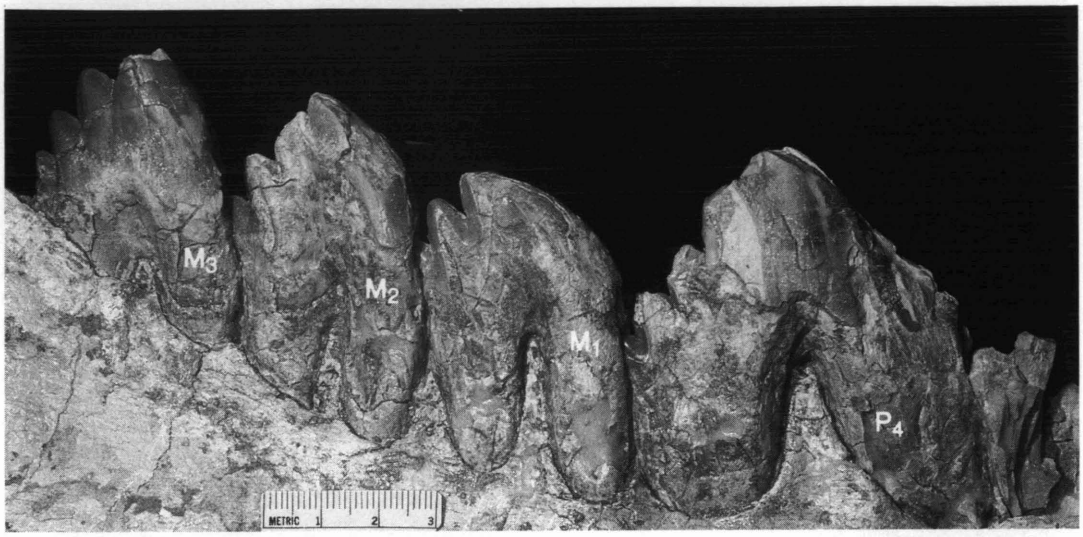

FIG. 12—Right lower premolars and molars of *Ancalecetus simonsi*, CGM 42290 (holotype), in lateral view. Scale is in cm. Note apical wear on the anterodorsal surfaces of all teeth (heaviest on M_{1-2}), and distinct lateral wear on the lateral surfaces of P_4-M_2 (there is no lateral wear on M_3). Heavy wear indicates that this individual lived to maturity. Heavy wear also indicates that *Ancalecetus*, like other basilosaurids, used its complex cheek teeth for mastication and not simply for manipulating food or straining plankton.

Figure 14, constructed on the assumption that *Ancalecetus simonsi* had 65 vertebrae similar in form to those of *Dorudon atrox*. This is possible, but it is also possible that *A. simonsi* had fewer vertebrae, in which case inferred positions in the column may be overestimated and the length-of-vertebrae profile in Figure 14 and our reconstructions in Figures 3 and 27A may be erroneously similar to those of *D. atrox*.

Cervix

There are seven cervical vertebrae in *Dorudon atrox* and we assume the same number to have been present in *Ancalecetus simonsi* although some were not recovered when the type was collected.

Atlas (C1).—The first cervical C1 (atlas; Fig. 15A) is the largest of the cervical vertebrae. It lacks a centrum and has the form of an oval ring surrounding the foramen magnum and articulating with the occipital condyles of the cranium. The neural arch is robust and about equal in craniocaudal length to the inferior arch. The inferior arch is dorsoventrally thicker than the neural arch and it supports both the cranial condylar articulations and the caudal articular surface. The ventral surface of the inferior arch is smooth, with a prominent backwardly-projecting hypapophysis. The neural canal is heart-shaped. There is a broad transverse process projecting laterally and caudally on both sides. The transverse process is narrow on its ventral surface and forms a broader, convex shelf on its dorsal surface. Transverse processes on each side are perforated by a small 4-5 mm foramen running craniocaudally that is seemingly too small to have carried a vertebral artery. Left and right vertebral arteries evidently went over rather than through the transverse processes. This course, or a course with a single penetration of the transverse process, is characteristic of basilosaurids, whereas vertebral arteries in protocetids penetrated a transverse process twice

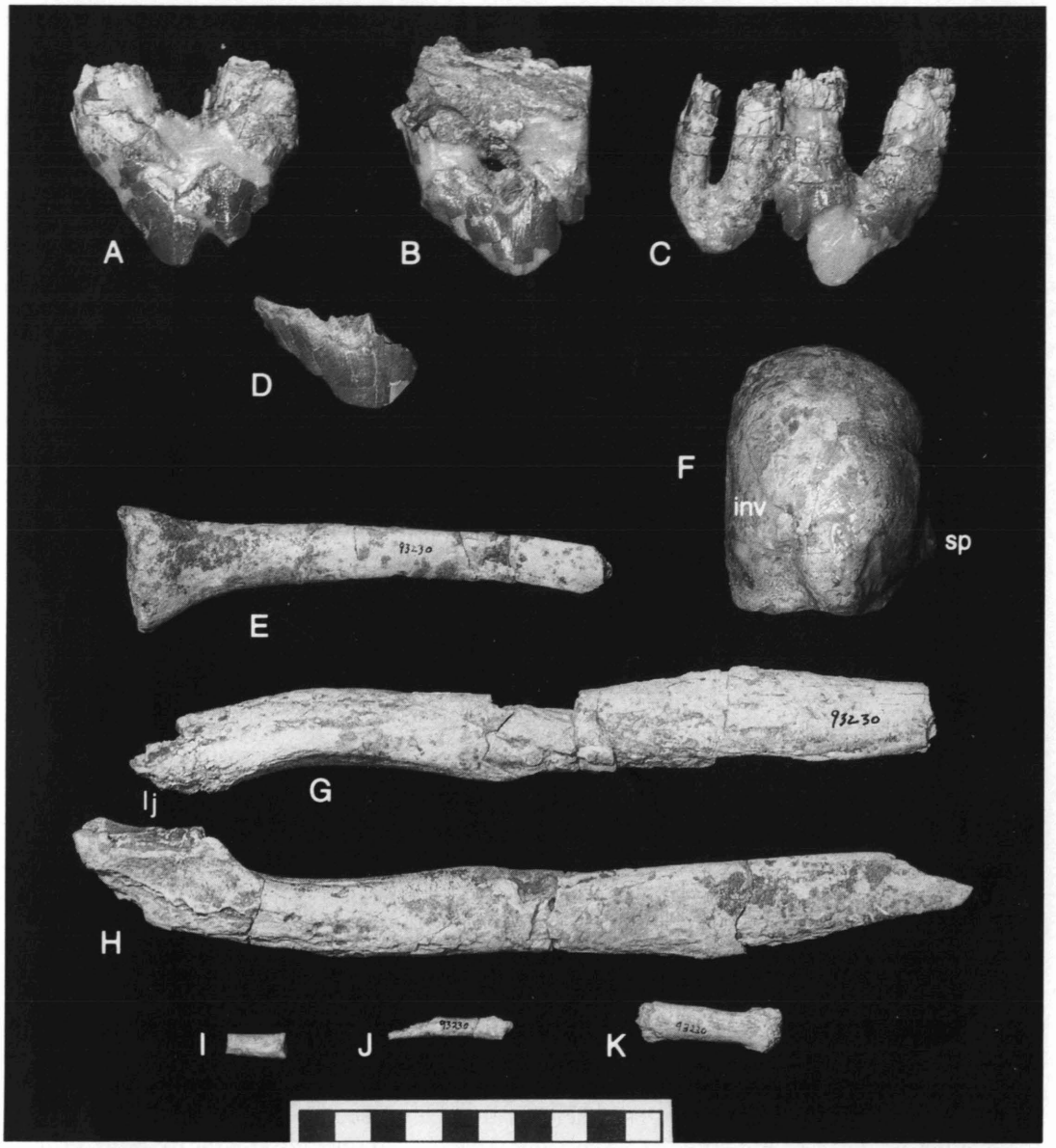

FIG. 13—Upper premolars, molars, thyrohyal, auditory bulla, jugals, and metacarpal of *Ancalecetus simonsi*, CGM 42290 (holotype). A, left P^3 in lateral view. B, left P^4 in lateral view. C, right M^1 and P^4 in lateral view. D, right P^3 in lateral view. E, right thyrohyal in lateral view. F, left auditory bulla in ventral view (anterior is at top, sigmoid process, **sp**, is opposite the involucrum, **inv**). G, left jugal in medial view (anterior is at left, dorsal edge is at bottom). H, right jugal in medial view (anterior is at left, dorsal edge is at top, and dorsal surface for articulation with lacrimal, **lj**, is at top left, followed by concave curvature of right orbit). I, phalangeal fragment? J, phalangeal fragment? K, right second metacarpal (Mc II) lacking distal epiphysis (dorsal view, base is at right). Scale is in cm. Note heavy wear on upper cheek teeth, and long lightly-built jugals like those of other advanced archaeocetes.

TABLE 3—Sizes of vertebrae of *Ancalecetus simonsi* in CGM 42290 (holotype; Figs. 14-16). Vertebral number given in parentheses, starting with C1 = 1, corresponds to that in Figure 14. Centrum length is measured ventrally. Centrum width and height are measured on the cranial face of the centrum. Asterisks mark estimates. Measurements are in mm.

	Centrum			Neural canal	
Vertebra	Length	Width	Height	Width	Height
C1 (1)	42.4	129.2	25.7	59.2	44.0
C2 (2)	40.2	108.0	29.7	38.0	24.7
C3? (3)	23.3	60.0	53.4	--	--
C7 (7)	28.1	69.9	56.3	34.8	32.3
T1 (8)	35.7	72.6	51.2	32.0	38.4
T2 (9)	42.8	67.1	46.8	51.6	34.1
T3 (10)	46.4	64.5	--	52.0	34.8
T4 (11)	46.5	65.7	50.3	52.2	--
T5 (12)	48.2	67.9	49.5	53.6	34.3
T6 (13)	51.2	68.5	50.3	54.1	29.2
T7 (14)	54.5	--	51.9	--	--
T11 (18)	55.2	84.7	60.4	49.4	35.4
T12 (19)	58.9	79.9	61.2	44.8	33.0
T14 (21)	59.5	84.0	65.0	45.6	33.4
T15 (22)	60.9	81.7	67.6	43.3	--
T16 (23)	60.0	78.9	--	--	--
T17? (24)	61.1	--	--	--	--
L12? (36)	60.1	82.0	73.0	43.0	34.8
Ca8 (52)	62.5	83.4	73.7	20.0	10.8
Ca14 (58)	37.6	66.9	65.4	--	--

before passing through a foramen in the neural arch to enter the foramen magnum and the braincase.

The cranial condylar articular surfaces are concave and kidney shaped. Their inferior edges are well separated by a narrow space on the inferior arch of the vertebra, while dorsal margins of the articular surfaces are well separated and connected to the neural arch by bony bridges that enclose lateral vertebral foramina some 8 × 10 mm in diameter for vertebral arteries. Caudal articular surfaces are flat, with dorsal edges being rounded. The functional length of the atlas, the minimum distance separating cranial condylar articular surfaces from caudal articular surfaces is 30 mm, which differs slightly from the measurement in Table 3 separating the middle parts of these articulations. The two caudal articular surfaces are confluent across the inferior arch, forming a notch for the dens of C2 (axis). In articulation, the neural arch of the atlas and pedicles of the axis form intervertebral foramina or openings that carried the first spinal nerve.

Axis (C2).—The axis (C2 in Fig. 15B) has the longest centrum of any of the cervical vertebrae. In addition, the dens or odontoid process projects anteriorly some 25 mm from the centrum to articulate with the inferior arch of the atlas. The dens is large and roughly conical, with a rounded apex. The caudal epiphysis is roughly oval in shape when viewed caudally, it

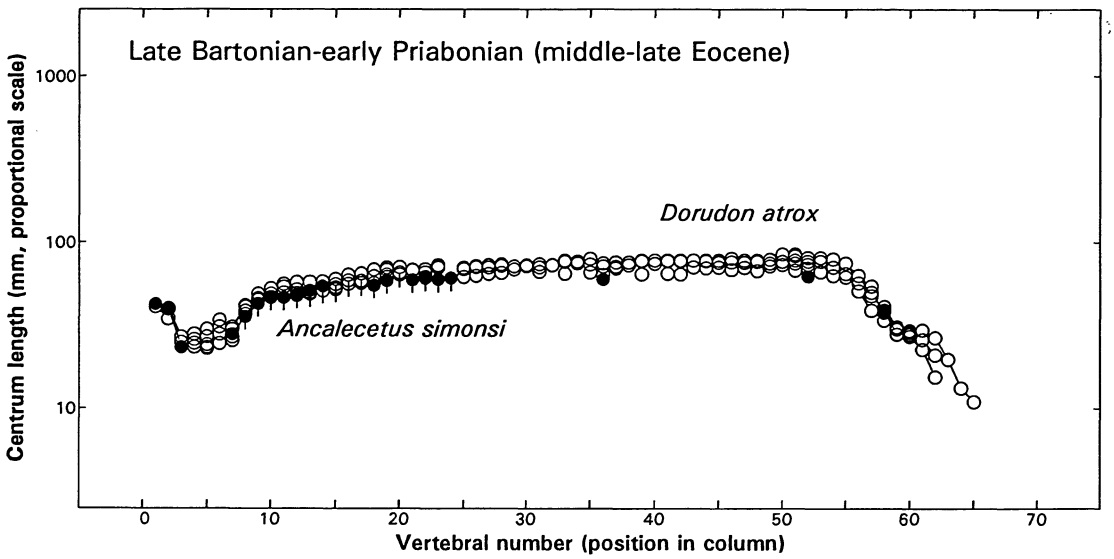

FIG. 14—Length-of-vertebrae profile for *Ancalecetus simonsi* (solid circles) from Wadi Hitan, based on vertebrae preserved in CGM 42290 (holotype; measurements in Table 3). This is superimposed on profiles for five specimens of late Bartonian to early Priabonian *Dorudon atrox* from Wadi Hitan (open circles). Measurements of *D. atrox* are from Uhen (1996, appendix D), and include CGM 42183 and UM 97512, 100146, 101215, and 101222. Note similarity of *A. simonsi* to *D. atrox* in thorax size (thoracic vertebrae in positions 8 through 24 are marked by vertical lines symbolizing ribs). Length-of-vertebrae profiles of *A. simonsi* and *D. atrox* appear similar, but identifications of lumbar and caudal vertebrae of *A. simonsi* are based on comparison to vertebrae of *D. atrox*—thus while it is possible both have similar profiles, there is no way to demonstrate this convincingly.

is deeply concave, and it bears two small ventral prominences separated by a central pit. The pedicles are large and angled relative to the midline of the vertebral column, but these are not as robust as the neural arch of the atlas. The neural spine is long craniocaudally at its base, and the base projects dorsally and cranially from the neural arch. The backward-projecting neural spine is broken just above this base. Postzygapophyses are high on the laminae and project caudally to articulate with prezygapophyses of C3. The postzygapophyses are angled such that their articular surfaces face somewhat laterally, caudally, and ventrally. Transverse processes enclose nutrient foramina some 4-5 mm in diameter. The transverse processes are divided distally, possibly reflecting the position of the vertebral arteries.

C3?.—A cervical vertebra is identified as the third or possibly fourth cervical by comparison with those of other basilosaurids. The centrum of this vertebra (Fig. 15C) is craniocaudally compressed and concave on both cranial and caudal ends. The cranial epiphysis is roughly oval in shape, but flattened along the dorsal and ventral margins. There is no hypapophysis present on the ventral surface of the centrum. The pedicles and neural arch are broken and not preserved. Transverse processes are broad, flattened craniocaudally, and perforated by large 1.6 × 0.8 mm vertebrarterial foramina just lateral to the centrum. Another fragment of a neural arch from C3, C4, or C5 (illustrated in Fig. 15C) is also present in CGM 42290.

C7.—The seventh cervical vertebra (C7 in Fig. 15D) is somewhat different from the other cervicals. The centrum is concave on both ends and it is the longest of all cervicals other than C2. Cranial and caudal epiphyses are shaped like flattened ovals. Pedicles are the most laterally expanded of all the cervical vertebrae. They are at a considerable angle to the midline of the body and confluent with the transverse processes, which project anteriorly as well as

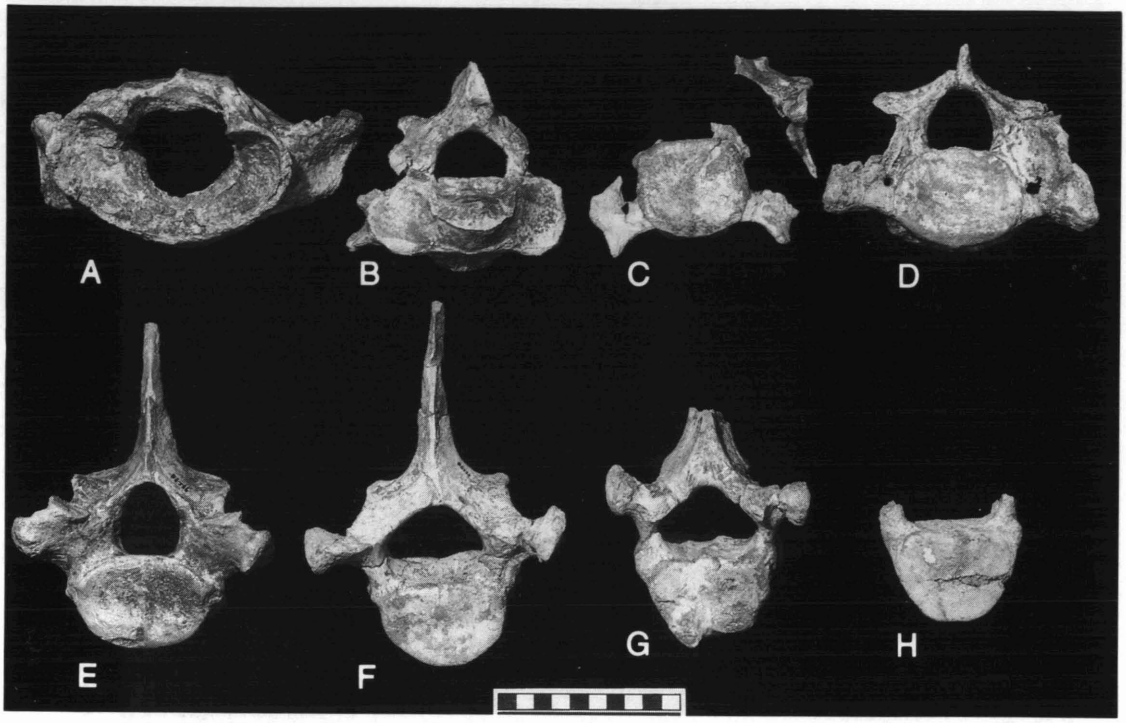

FIG. 15—Cervical (A-D) and anterior thoracic (E-H) vertebrae of *Ancalecetus simonsi*, CGM 42290 (holotype). A, C1 (atlas). B, C2 (axis). C, C3?. D, C7. E, T1. F, T2. G, T3. H, T4. All are shown in anterior view. Scale is in cm.

laterally. Transverse processes are perforated by a foramen 6 mm in diameter, which seems too small to carry a vertebral artery but is in the position of the vertebrarterial canal. The pedicles join craniocaudally-thin laminae to form the neural arch enclosing the neural canal. Prezygapophyses are angled dorsally and slightly medially, while postzygapophyses are angled ventrally and slightly laterally.

Thorax

Thoracic vertebrae are rib-bearing. These number seventeen in *Dorudon atrox* and the same number may have been present in *Ancalecetus simonsi* although we cannot demonstrate this.

T1, T2, T3, and T4.—The first through fourth thoracic vertebrae (**T1-T4** in Fig. 15E-H) are the shortest of the thoracic vertebrae. Centra increase in length and height from T1 to T4, but remain relatively constant in breadth. The centrum of T1 is especially wide relative to its height. Centrum surfaces become more nearly equant (height equaling width) as one proceeds down the column. All centra are moderately waisted (bearing ventrolateral depressions). T1 and T2 are complete, T3 is missing much of the neural spine, and T4 is missing the entire neural arch. The lateral edge of each caudal epiphysis turns cranially onto the lateral face of the centrum to form the anterior edge of a prominent fovea for the head of each rib. These foveae are much more prominent than those associated with cranial epiphyses.

Pedicles of T1 to T4 are very long and robust, and these undergo some reorientation, moving from T1 to T4, as a more mediolateral alignment gives way to a more craniocaudal orientation. Dorsal edges of the pedicles are connected to laminae, which together form the neural arch. Neural canals are large, and each has a relatively flat ventral border along the

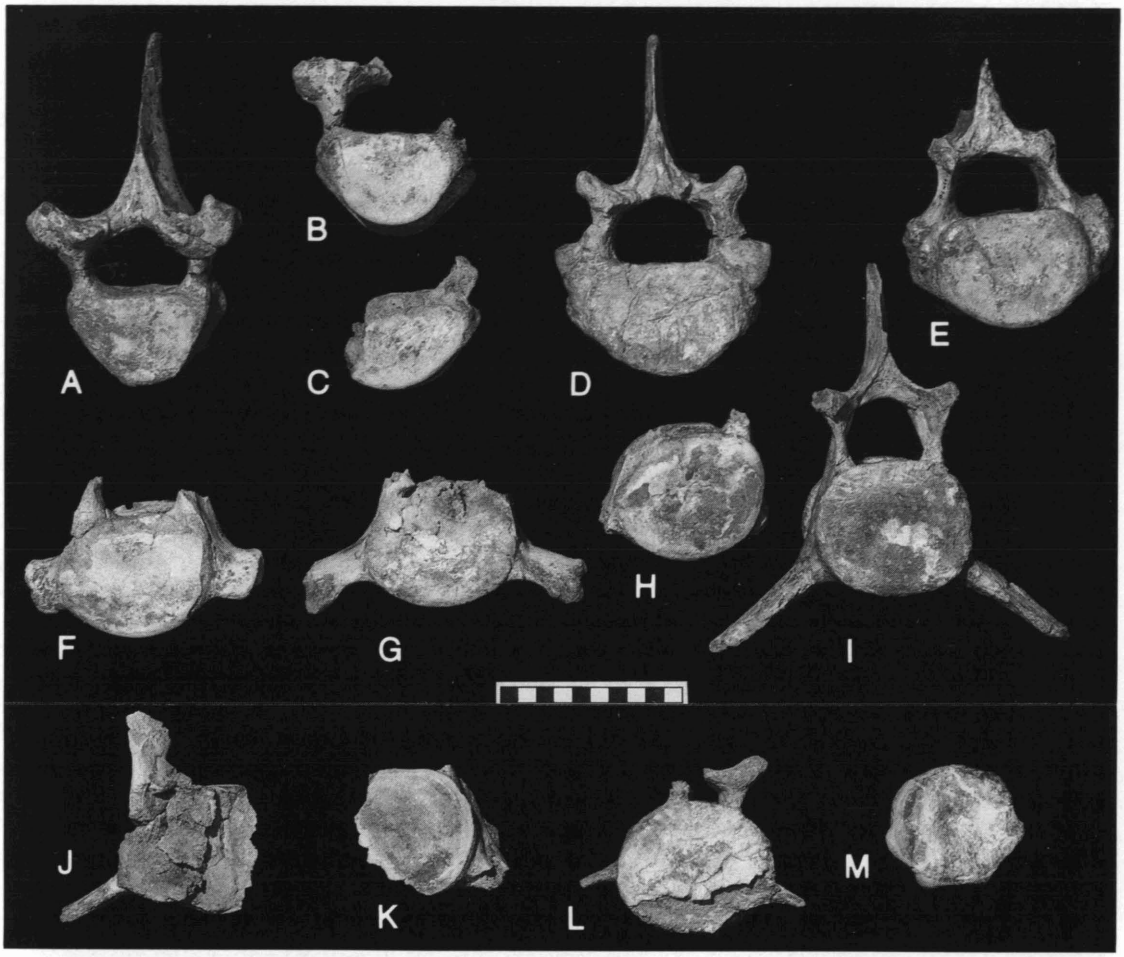

FIG. 16—Thoracic, lumbar, and caudal vertebrae of *Ancalecetus simonsi*, CGM 42290 (holotype). A, T5. B, T6. C, T7. D, T11. E, T12 (T14, not shown, is similar). F, T15. G, T16. H, T17?. I, L12? J, unidentified lumbar. K, unidentified lumbar. L, Ca8. M, Ca14. All are shown in anterior view. Scale is in cm.

dorsal surface of each centrum. The dorsal border of the neural canal rises to a rounded apex where laminae join along the midline of each vertebra. Adjacent vertebrae enclose an intervertebral foramen or space.

The neural spine on T1 is relatively short and gracile, but that on T2 is both longer and more robust. Prezygapophyses are oval in shape and inclined slightly medially and slightly anteriorly. Postzygapophyses extend posteriorly from the laminae and are flat, oval, and inclined slightly laterally and slightly posteriorly. Transverse processes of T1 to T3 arise from the tops of pedicles and bear circular foveae for rib tubercula. There is a slight ventral keel on T1 that is entirely absent on T2-T4.

T5, T6, and T7.—Thoracic vertebrae T5 to T7 (Fig. 16A-C) are larger than T1 to T4 and also similar to each other. T5 is virtually complete. T6 is a complete centrum with part of a neural arch, while T7 is part of a damaged centrum lacking the neural arch altogether. The centra are about as high as they are long, while the width is greater than either of these measurements. The centra again are waisted, with their narrowest constriction at approximately

mid-length. Cranial epiphyses are roughly heart-shaped, reaching their greatest width just below the site for articulation with rib capitula. A small protuberance is present on the dorsolateral edge of the centrum, just lateral to the widest point of the cranial epiphysis on each vertebra that forms the posterior edge of the fovea for the rib capitula. This protuberance is not covered by the cranial epiphysis. Caudal epiphyses of T5 to T7 are slightly wider than their cranial counterparts, but similar in shape. The caudal epiphyses extend onto the lateral faces of the centra, covering a caudolaterally-facing depression on each vertebra. These foveae accept the heads of ribs that correspond in number to the vertebra behind them.

Pedicles rise from the centra just dorsal to the rib articular surfaces and angle slightly cranially. The dorsalmost extensions of the pedicles meet with the laminae to form the neural arches. Laminae of T5 angle dorsally toward the midline, where they meet and form the base of the neural spine. The neural canal passing through the neural arch is broader than it is high. The bases of the neural canals of T5 to T7 are rather flat when compared to the dorsal border of the neural canal of T5, which is more rounded. Caudal intervertebral notches of T5, forming the anterior border of the intervertebral foramen or space, are deeply excavated into the caudal borders of the pedicles.

The neural spine of T5 is broader, higher, and less inclined than those of T1 or T2. The dorsal tip of the neural spine of T5 comes to an abraded rounded point. The anterior face of the base of the neural spine is roughly triangular in shape. The base of the triangular surface is formed by the dorsal edge of the neural arch. Paired low ridges originate at the base of the triangular space and angle medially to meet at a point. These ridges delimit three fossae. One is triangular along the midline, the others are a pair of broad grooves that meet along the midline. Dorsal to this complex area, the cranial border of the neural spine is a simple sharp ridge. The caudal border of the neural spine is divided into three parts: a caudally projecting midline ridge, and two lateral ridges. All of these ridges are pronounced, but the midline ridge projects farther caudally than do the lateral ridges. These ridges define a pair of fossae on each vertebra on either side of the midline for attachment of epaxial muscles.

Prezygapophyses of T5 arise from the neural arch where the pedicles and laminae meet. They are large and project anteriorly. Articular surfaces on the prezygapophyses are somewhat damaged on T5. Prominent metapophyses are positioned lateral to and above the prezygapophyses on the dorsal part of each transverse process, forming attachment surfaces for epaxial muscles. Postzygapophyses extend caudally from the laminae of T5. These are flat and almost horizontal. The transverse processes of T5 project cranially and dorsally from the junctions of the pedicles and laminae. These are very short and thick, and support foveae for rib tubercula on their lateral surfaces. Thoracic vertebrae five to seven lack ventral keels.

T11 and T12.—Thoracic vertebrae T11 and T12 (Fig. 16D-E) are similar in size. Centra are approximately as long as they are high, but they are much wider than high or long. These are somewhat waisted, but less so than more anterior thoracics. The fovea for the rib capitulum projects from the lateral side of the centrum at its widest point. Cranial epiphyses are broadly oval in outline and much wider than the cranial epiphyses of more anterior thoracic vertebrae. Caudal epiphyses too are broadly oval.

Pedicles rise nearly vertically from the centra. Laminae angle dorsally from their junction with the pedicles toward the midline of the neural arch and the base of the neural spine. The neural arches of T11 and T12 are broadest at their bases. The caudal borders of pedicles are not deeply incised like more anterior vertebrae, but the pedicles do not extend to the caudal end of the centrum, thus allowing space between adjacent pedicles for passage of spinal nerves.

The neural spine of T11 is intact but that of T12 is damaged. The anterior face of the base of the neural spine on T11 is triangular in shape, coming to a point dorsally. The base of the triangular surface is formed by the dorsal edge of the neural arch. A pair of low ridges originate at the base of the triangular space and angle medially to meet at a point. These ridges delimit three fossae. One is triangular along the midline, the others are a pair of broad grooves

that meet along the midline. Viewed dorsally, the spines are wedge-shaped in cross section, with a sharp anterior border flaring laterally along the caudal border of each vertebra.

Prezygapophyses arise from the neural arch at the junction between the pedicles and laminae on each vertebra and are angled inward at about 45°. Metapophyses are high and project both laterally and cranially. Postzygapophyses project caudally from the ventral edge of the caudal border of the neural spines. The articular surfaces of the postzygapophyses angle ventrolaterally and are convex rather than flat. Transverse processes of T11 rise from the bases of the pedicles and from the centrum itself. The two rib articular surfaces are close to each other, but have not merged into a single fovea. T12 on the other hand appears to have a single rib facet, but it is also damaged.

T14, T15, T16, T17?.—Thoracic vertebrae T14 to T17? (Fig. 16F-H; T14 is not illustrated) are the final vertebrae in the thoracic series. All are damaged. T14 includes the centrum, transverse process, and neural arch, but it is missing much of the neural spine, prezygapophyses, and metapophyses. T15 and T16 are missing the entire neural arch and T17? is only a centrum. This vertebra is the right size to articulate with T16, but it may be an anterior lumbar. The centra are about as long as they are high, but they are wider than they are high or long. Cranial epiphyses are generally oval in outline, but these are slightly flattened on their dorsal margins. Cranial epiphyses become progressively more circular from T14 to T17?. The caudal epiphyses are similar in shape to their cranial counterparts. They too become more circular from T14 to T17?.

Pedicles rise almost vertically from the lateral edges of the dorsum of each centrum. They are somewhat shorter than the vertebral centra, and their cranial margins are closer to the cranial end of each vertebrae than their caudal margins are to the caudal end of each vertebra. The pedicles meet the laminae to form the neural arches. Laminae of T14 are rather short, and angle dorsally from the top of the pedicles to the midline of the neural arch at the base of the neural spine on each vertebra. The floor of the neural canal is generally flat, but there is a longitudinal ridge running down the midline, flanked by nutrient foramina on each side. The top of the neural canal comes to a broadly rounded point where the laminae meet along the midline. Caudal intervertebral notches are not deeply incised into the caudal borders of the pedicles, but the pedicles are some distance from the caudal end of each centrum, leaving space for passage of spinal nerves. There is a variably distinct groove developed in the centrum of each vertebra between the caudal border of the pedicle and the caudal epiphysis.

Neural spines and prezygapophyses are poorly preserved or missing on T14 through T17?. Transverse processes increase dramatically in length from T14 to T16. Transverse processes are short and stout on T14, but as they lengthen they also become thinner. The transverse processes of T14 and T15 are approximately horizontal, but the longer processes of T16 angle ventrally. None of the transverse processes angle significantly cranially or caudally. These vertebrae all have a single articular surface for rib articulation on the ends of the transverse processes (this cannot be seen on T17? due to breakage).

The ventral side of the centrum of each vertebra includes a distinct ventral keel on the midline, flanked by a pair of nutrient foramina, one on each side of the keel. These foramina are variably developed, with one foramen often much better developed than the other, or with one missing altogether. There is also a pair of accessory ridges lateral to the nutrient foramen that parallel the ventral keel. These accessory ridges are always smaller than the midline keel, but are similar in form.

Lumbus

There are some twenty lumbar vertebrae in *Dorudon atrox* and the same number may have been present in *Ancalecetus simonsi*. However the lumbus and cauda are poorly preserved and we cannot demonstrate this.

L12?.—Several partial centra of lumbar vertebrae are associated with CGM 42290, but a single lumbar vertebra, possibly L12, is sufficiently well preserved to warrant description (Fig. 16I). The centrum is oval in cross-section and it is about as long as it is high. The dorsal surface of the centrum has a ridge running down the midline, on the floor of the neural canal, with a single nutrient foramen on the right side of the ridge. The ventral surface of the centrum is perforated by a pair of nutrient foramina, close to the midline, one on either side of a ventral keel. Cranial epiphyses are nearly circular in outline, but the shape is slightly flattened on the dorsal edge. The cranial epiphysis is generally flat with a slight indentation in the center. The caudal epiphysis is oval in outline, but lacks the distinctly flattened dorsal edge of the cranial epiphysis. The caudal epiphysis is also generally flat with a slight indentation in the center.

Pedicles are thin and meet the laminae to form the neural arch. The neural canal is large, with an arched profile. The intervertebral foramen or space is formed by the posterior border of the pedicle and the anterior border of the pedicle of the following vertebra. At the ventral edge of each intervertebral foramen there is a shallow but distinct groove on the centrum between the posterior edge of the pedicle and the posterior epiphysis. The neural spine is broad at its base, but broken distally. Small metapophyses project anteriorly and dorsally from the neural arch. These resemble prezygapophyses superficially, but there is no longer a zygapophyseal contact between adjacent vertebrae this far back in the vertebral column. Transverse processes are longer than those of thoracic vertebrae, but much less robust. These are thick at their bases but thin laterally. The distal ends of the transverse processes are flat with a rounded edge. Transverse processes are angled ventrally and slightly cranially.

Cauda

There are usually twenty-one caudal vertebrae in *Dorudon atrox* and the same number may have been present in *Ancalecetus simonsi*, although the tail is poorly preserved and we cannot demonstrate this. Anterior caudal vertebrae are separated from posterior lumbars in most mammals by a sacrum comprising one or more fused vertebrae that articulate with innominate bones of the pelvic girdle. When a sacrum is lacking, as it is here and in most cetaceans, anterior caudals are distinguished from lumbars by the presence of posteroventral facets for articulation with hemapophyses (hemal arches or chevron bones). No chevron bones are preserved in CGM 42290, but Ca8 has chevron facets indicating that it is an anterior caudal.

Ca8.—Caudal vertebra Ca8 (Fig. 16L) has a centrum that is longer than it is high or wide. The centrum is shallowly concave on both ends. The cranial epiphysis is oval in outline, being wider than it is high, as is the caudal epiphysis. The pedicles are located well forward on the centrum. They are very short anteroposteriorly, while the laminae are thin and relatively long. Pedicles and laminae together formed a neural arch enclosing a neural canal of small diameter (the right side and middle of the arch are broken). The transverse processes extend laterally a short distance from the lower part of the centrum. These are angled caudally and perforated on each side by a foramen for a spinal artery. Paired chevron articulations are present on the ventral side of the centrum at its caudal end.

Ca14.—Caudal vertebra Ca14 (Fig. 16M) is wider than it is high. The centrum is very waisted, and constriction of the centrum forms a deep groove around the circumference of the body. The cranial epiphysis of Ca14 is nearly circular in outline, being only slightly wider than it is high, and the caudal epiphysis is nearly circular as well, but smaller in area than the cranial epiphysis. The caudal epiphysis has a slight concavity in the center but its outer edges are convexly rounded. There is no trace of a neural arch nor remnant of a neural canal.

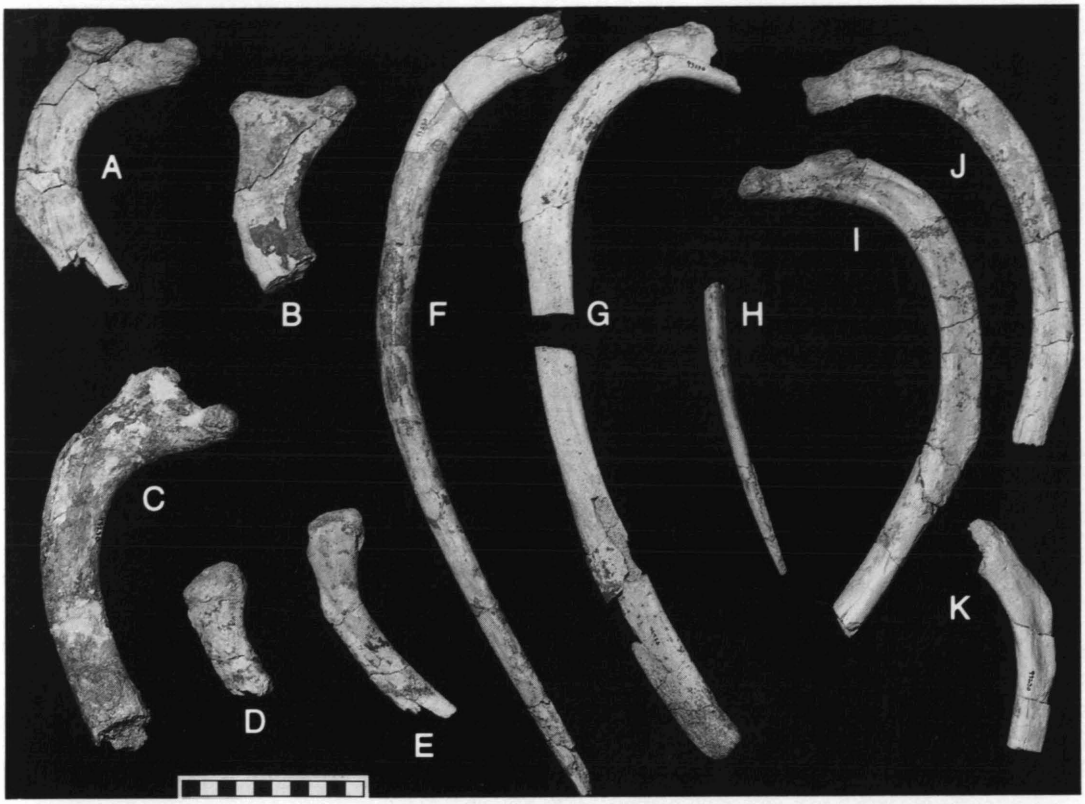

FIG. 17—Ribs of *Ancalecetus simonsi*, CGM 42290 (holotype), in various views. Scale is in cm. A-C, anterior ribs. D-H, posterior ribs. I-K, middle ribs. These ribs are typical of those found in *Dorudon atrox* and other basilosaurids of similar size.

Ribs and Sternum

Ribs.—There are parts of at least eleven ribs preserved in CGM 42290 (Fig. 17A-K), out of a possible total of 34 (if the vertebral column had 17 thoracic vertebrae). As in other basilosaurids, anterior ribs are robust, with the capitulum and tuberculum well separated and the body tightly curved. Middle ribs are more lightly built, with the capitulum and tuberculum closer together and the body straighter. Posterior ribs are slender, have a capitulum but no tuberculum, and are generally almost straight. Pieces of ribs from all regions of the thorax are present in CGM 42290. There is no indication of expansion of the distal ends of ribs nor of the pachyostosis that is sometimes found in other advanced archaeocetes (Buffrénil et al., 1990).

The rib illustrated in Figure 17B, possibly a first rib, has a body measuring 38.8 × 12.2 mm in diameter. The body of the more posterior rib illustrated in Figure 17F measures 27.4 × 12.4 : 19.2 × 16.1 : 17.0 × 10.9 mm, respectively, proximally, at the midshaft, and distally.

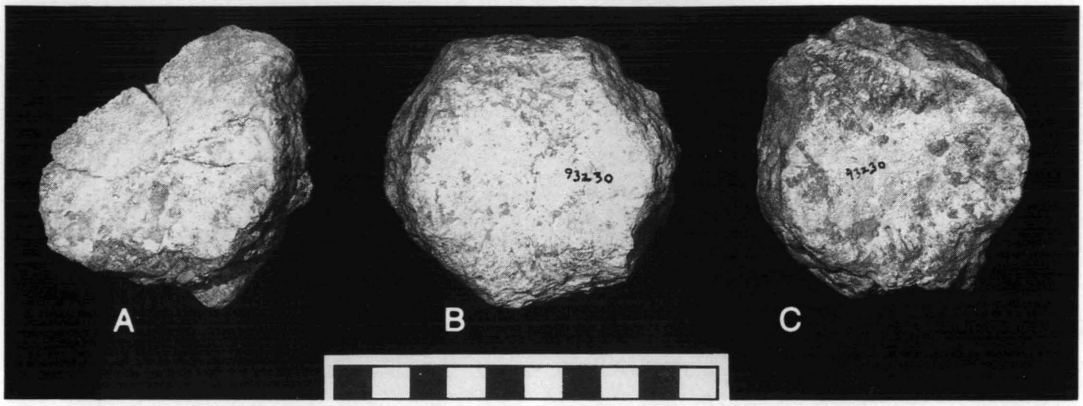

FIG. 18—Sternal elements of *Ancalecetus simonsi*, CGM 42290 (holotype), in dorsal view. Manubrium and xiphisternum were not found. Scale is in cm. These mesosternal elements are thick dorsoventrally and composed of spongy bone like those found in *Dorudon atrox* and other advanced basilosaurids of similar size.

Sternum.—Three sternal elements are preserved in CGM 42290 (Fig. 18A-C), all part of the mesosternum. The manubrium or presternum is not preserved, nor is the xiphisternum. The texture of bone is spongy within the one sternal element that is broken, suggesting that these could not have contributed significantly to neutralize buoyancy (Buffrénil et al., 1990). The best preserved of the three mesosternal elements measures about 75 mm in anteroposterior length, 69 mm in transverse width, and 35 mm in dorsoventral height.

Brachium

The forelimb of *Ancalecetus simonsi* is the most distinctive part of its anatomy, and this is very different from the forelimbs of all archaeocetes known previously. *A. simonsi* even lacks some features commonly used to characterize Cetacea as a group (e.g., it lacks a broad scapula, and an enarthrosis or ball-and-socket shoulder joint permitting broad excursion). The forelimb of *Ancalecetus* has an unusual orientation relative to the rest of the body, as shown in Figures 3 and 27A, and little ability to alter this, which is the reason we use the terms dorsal and ventral rather than posterior and anterior, respectively, in description of many forelimb elements.

Scapula.—Parts of both scapulae are preserved in CGM 42290. The left scapula (Sc in Fig. 19) is the better preserved. The scapular blade is very narrow anteroposteriorly when compared that of any other cetacean. As a consequence of this narrowness, the vertebral or dorsal border of the scapula is curved on a tight radius rather than being broadly arced as in other cetaceans. The scapular blade thins toward the vertebral border, and this border has a roughened edge indicative of some cartilaginous extension. Most modern cetaceans have cartilage along the entire vertebral border, extending the surface of the scapular blade, and this was probably true in *Ancalecetus simonsi* as well. However, the cranial border of the scapula has a smoothly rounded edge that is thicker than the vertebral border, and close to the glenoid this thickens even more. The caudal border is similarly rounded, and it too becomes thicker near the glenoid.

There is a scapular spine (s), but this is rather low and rounded. It divides the lateral surface of the scapula into a supraspinous fossa (ssf; cranial to the spine) and an infraspinous fossa (isf; caudal to the spine). The height of the spine above the lateral surface of the blade decreases from the base of the acromion process to the dorsal margin of the scapula where it

merges into the surface of the blade. The supraspinous fossa is less than half the area of the infraspinous fossa. The latter is relatively much smaller than the infraspinous fossa of other cetaceans. In most cetaceans, including other archaeocetes, the caudal border of the scapula curves posteriorly, giving the infraspinous fossa and the teres fossa together a large surface of attachment. In *Ancalecetus simonsi* the caudal border is not curved and the scapular blade is very narrow. No distinct teres fossa can be identified in CGM 42290.

The glenoid cavity of the scapula (gc) is oval in outline and very shallow. It faces posteriorly rather than ventrally as in other cetaceans. The surface of the concavity is somewhat irregular, rather than smooth, and articulation with the humerus shows that there was very limited motion possible at this joint. The acromion process (ac) is unusual. This is normally directed anteriorly in cetaceans, but in *A. simonsi* it is folded over to point ventrally and posteriorly, so that what would have been the lateral surface of the process in a conventional cetacean now faces medially (this is a description of the form of the acromion, not an interpretation of how the process came to be oriented this way). The medial side of the acromion bears a distinct process (hpa in Fig. 20) projecting toward the glenoid cavity and this process appears to have had ligamentous connection to a fovea on the humeral head. The acromion itself is separated from the glenoid by a deep groove. The coracoid process (cp) is rather short and stout, extending ventrally and anteriorly from its base on the neck of the scapula. There are two protuberances on the medial side of the coracoid process that do not have known homologs nor obvious functions.

Measurements of the scapula are L = 276 mm (over coracoid process); MLW = 3.6 : 11.9 : 43.0 mm (the latter is measured to include the glenoid plus the acromion); APH = 170 : 33.9 (narrowest point): 77.1 mm (over coracoid plus acromion).

Humerus.—The humerus (H in Fig. 19) of *Ancalecetus simonsi* is also very different from that of other basilosaurids. The body of the humerus is relatively flat and the head is relatively small. The proximal half of the medial wall of both humeri appears to have collapsed when it was buried, suggesting that the internal trabecular structure may not have been as strong as that of other contemporary basilosaurids. The head (h in Figs. 19-20) has one main articular surface. This is oval in outline, slightly convex, and faces dorsolaterally. Its surface is smooth, and it clearly articulated with the glenoid fossa of the scapula. There is a second surface of note on the anterolateral side of the head. This too is ovate but it bears a distinct fovea (the capitular fovea of the humerus, cfh in Fig. 20) that appears to have been connected to the humeral process of the scapular acromion (hpa in Fig. 20) by a ligament.

The greater tuberosity (gt) of the humerus is a large surface on the ventral side of the proximal humerus separated from the head by a shallow but conspicuous groove. The deltopectoral crest (dpc) is a prominent ridge of bone that runs from the greater tuberosity to a point about 5 cm from the distal end of the humerus, projecting ventrally from the body. The greater tuberosity is similar in position and shape to that of other basilosaurids, but it is not nearly as large. The lesser tuberosity (lt) is a large surface on the medial side of the humerus. It is separated from the humeral head by a shallow sulcus, and from the greater tuberosity by a deeper but ill-defined bicipital groove. The distal end of the humerus is unusual, with a textured flat posterodistal surface (recall the unusual orientation of the forelimb in life as shown in Fig. 3) for articulation with the radius, and a textured flat distal surface for articulation with the ulna. The contacts of humerus to radius and ulna, whether fused as these are on the left side, or tightly fitting but separate as these are on the right side, permitted no motion between bones at the elbow joint.

Measurements of the humerus are L = 195 mm; MLW = 46.2 (head plus lesser tuberosity): 20.5 : 26.0 mm; DVH = 34.5 : 67.8 : 36.5 mm.

Ulna.—The ulna (U in Figs. 19 and 21) of *Ancalecetus simonsi* is very different from that of other basilosaurids in lacking a trochlear notch and in having a reduced olecranon. The part of the ulna that is trochlear notch in other basilosaurids is here a textured flat surface that is solidly joined with a complementary surface on the distal end of the humerus. Contact with

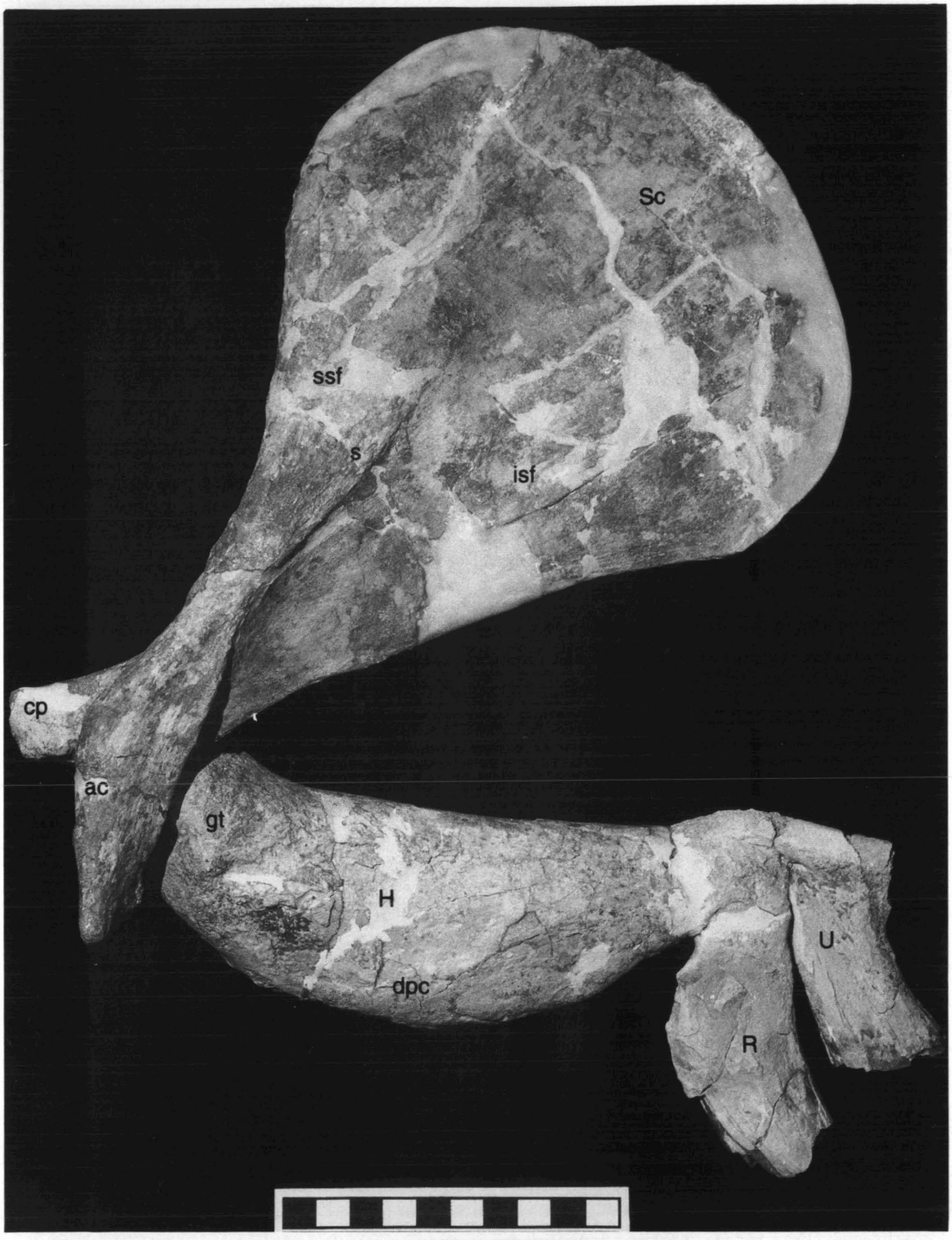

FIG. 19—Left scapula and partial forelimb of *Ancalecetus simonsi*, CGM 42290 (holotype), in lateral view. Scale is in cm. Note the narrow scapular blade, ventrally-projecting acromion process, unusual angle of articulation of the scapula and humerus, and fusion of the radius and ulna to the distal humerus. Abbreviations are given in the facing caption for Figure 20.

FIG. 20—Detail of articulation of the left scapula and humerus of *Ancalecetus simonsi*, CGM 42290 (holotype). Both bones are shown in oblique lateral views with the joint opened to show articulating surfaces. Abbreviations from Table 1 are: **ac**, acromion process; **cfh**, capitular fovea of humerus; **cp**, coracoid process; **dpc**, deltopectoral crest of humerus; **gc**, glenoid cavity; **gt**, greater tuberosity of humerus; **h**, head of the humerus; **H**, humerus; **hpa**, humeral process of the acromion; **isf**, infraspinous fossa; **lt**, lesser tuberosity of humerus; **R**, radius; **s**, spine of the scapula; **Sc**, scapula; **ssf**, supraspinous fossa; **U**, ulna. Scale is in cm.

the radius is limited to the most-proximal centimeter or less of their parallel course. The olecranon process is reduced to a small tubercle that projects dorsally from the dorsal border of the ulna. The body of the ulna is mesiolaterally narrow at the proximal end, and it becomes broader distally. This is different from the conformation of the ulnar body in other advanced basilosaurids, which are usually broad along their entire length. The broad distal end of the ulna articulates with the pisiform, cuneiform, and lunar along a highly irregular surface, meaning that the articulations cannot have been synovial (see below).

Measurements of the ulna are L = 143 mm; MLW = 26.3 : 21.6 : 27.4 mm; DVH = 32.3 : 35.1 : 45.1 mm.

Radius.—The radius (**R** in Figs. 19 and 21) has a textured flat proximal surface for articulation with the complementary posterodistal surface of the humerus. The proximal part of the radius is compressed in conformity with the plane of the forelimb. This is different from the condition in other basilosaurids, which all have circular proximal radii. The ulnar margin of the radius is flattened where it parallels the ulna, while the opposite (ventral) margin of the radius is narrower and rounded. The distal radius is more like that of other basilosaurids. It has an articular facet on the ulnar side for the lunar, and another for the scaphoid. Neither of

FIG. 21—Right forelimb and carpus of *Ancalecetus simonsi*, CGM 42290 (holotype), in lateral view. Abbreviations from Table 1 are: **H**, humerus; **R**, radius; **U**, ulna. Scale is in cm. Here again the radius and ulna are solidly fused to the distal humerus. Note the relatively small size of carpal bones.

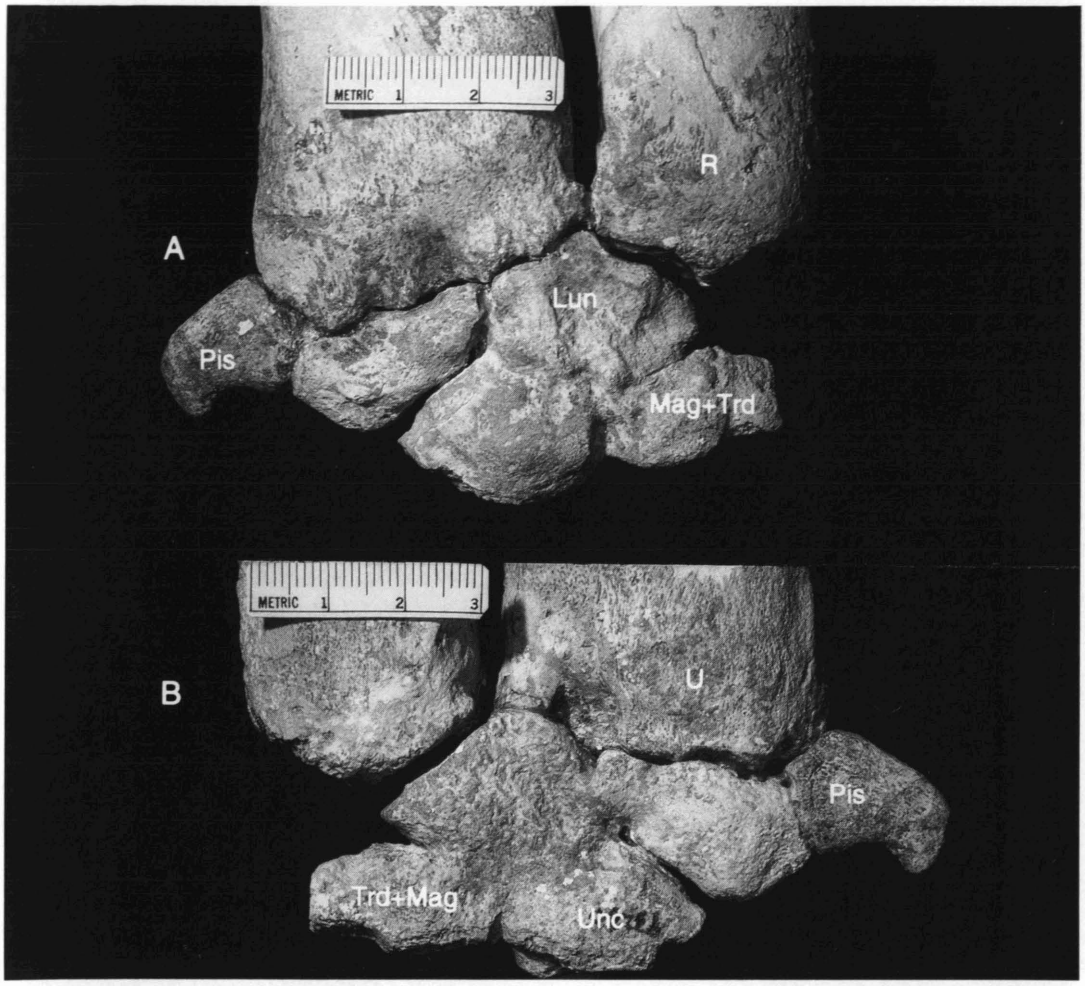

FIG. 22—Right carpus of *Ancalecetus simonsi*, CGM 42290 (holotype) in lateral (A) and medial views (B). Abbreviations from Table 1 are: **Cun**, cuneiform; **Lun**, lunar; **Mag**, magnum; **Pis**, pisiform; **R**, radius; **Trd**, trapezoid; **U**, ulna; **Unc**, unciform. Carpals shown here were all found as shown here, fused to the distal radius and ulna. There is a conspicuous space for a scaphoid between the radius and fused magnum-trapezoid, but the scaphoid itself was not found. It is not clear whether a trapezium was present in life. Scales are in cm.

these facets are particularly smooth, although they may have retained some vestige of a synovial joint surface.

Measurements of the radius are L = 137 mm; MLW = 21.4 : 17.1 : 21.8 mm; DVH = 43.3 : 34.6 : 31.8 mm.

Manus

The hand of *Ancalecetus simonsi*, as preserved, includes six separate bones and indications of at least five others. Four of the preserved bones are block-shaped carpals, and both of the indicated missing bones are also carpals. The four that are known are tightly packed and ar-

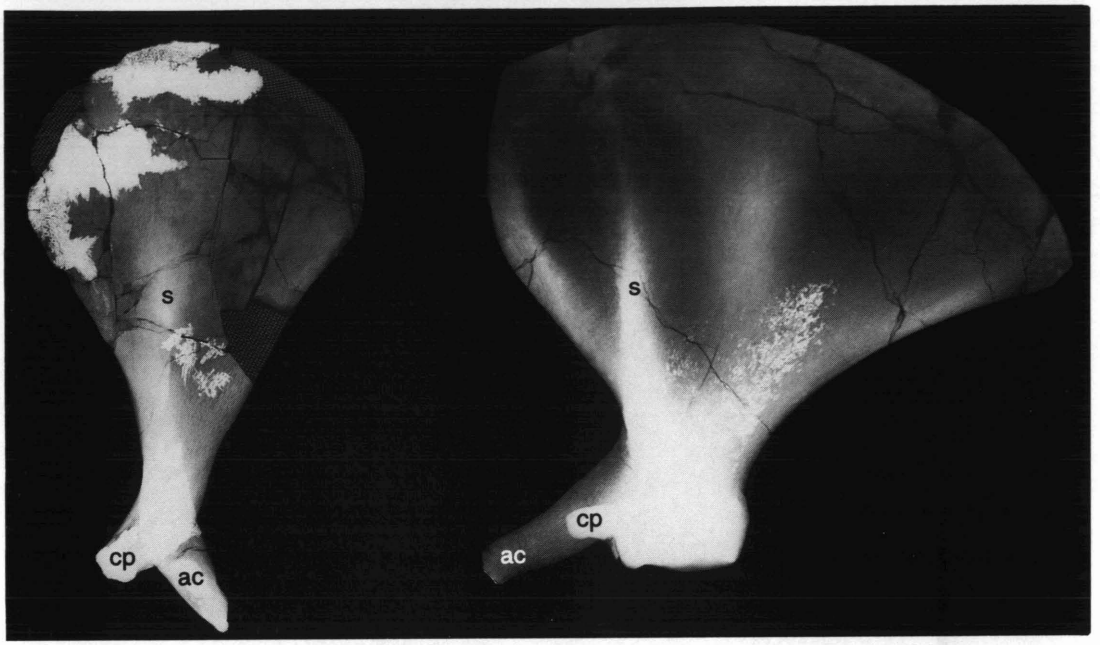

FIG. 23—Radiographic comparison of the left scapula of *Ancalecetus simonsi*, CGM 42290 (holotype) with the left scapula of *Dorudon atrox*, UM 100222, showing how these differ in shape. Both are illustrated at about 1/3 natural size. Abbreviations from Table 1 are: **ac**, acromion process; **cp**, coracoid process; **s**, spine of the scapula. Note the absence of any evident pathology that might explain the unusual shape of the scapula or pattern of development and fusion seen in forelimbs of *Ancalecetus*. Bright white in this and other radiographs is barite permineralization that is opaque to x-rays.

ranged in a proximal and a distal row that originally had three bones each. Carpals in the two rows are not arranged serially but rather alternate with each other. The fifth preserved bone of the hand is the pisiform, a sesamoid, which articulates with the ulna and cuneiform on the dorsal side of the manus (recall the unusual orientation of the forelimb in life as shown in Fig. 3; dorsal here means toward the pisiform, and medial here means palmar; lateral would be dorsal in normal anatomical position if the forelimb could be pronated). The sixth preserved bone of the hand is one of at least four metacarpals present in life in the hand of *A. simonsi*.

Scaphoid.—The scaphoid is the most ventral carpal in the proximal row. It is not preserved in CGM 42290, but was almost certainly present in *Ancalecetus simonsi*. There is an articular surface on the ventral edge of the distal radius for a scaphoid. Since the scaphoid itself is missing, and the articular surface on the radius is not broken, the scaphoid was probably not fused to the radius nor to any of the other known carpals. The trapezium is also missing, so it is unclear whether or not the scaphoid might have been fused to it.

Lunar.—The lunar (Lun in Fig. 22) is the central carpal in the proximal row. It articulates with the radius and ulna proximally, the scaphoid ventrally, the cuneiform dorsally, and the unciform and magnum part of the magnum-trapezoid distally. It is free from the radius and scaphoid, but is fused to some extent to all of the other bones with which it makes contact. It is most firmly fused to the unciform and trapezoid, and has small areas of fusion to the ulna and cuneiform. Articular surfaces that are not fused are textured rather than smooth.

The lunar measures about 17.6 mm proximodistally, 31.2 mm dorsoventrally, and 16.5 mm mesiolaterally.

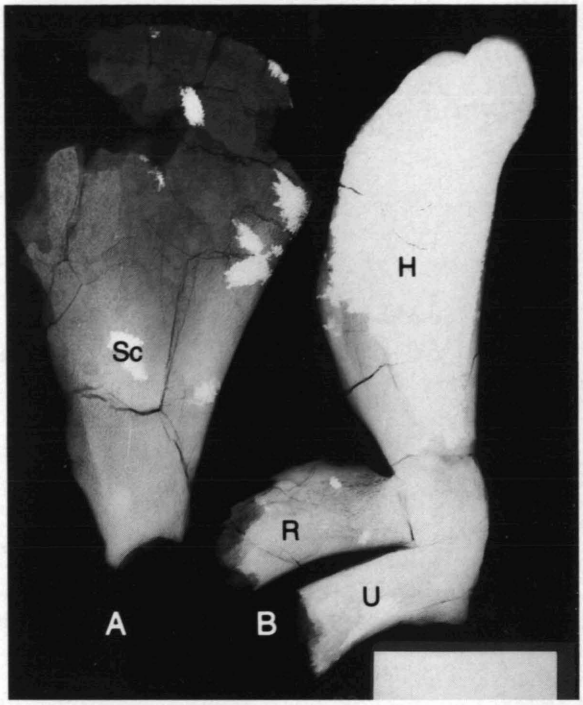

FIG. 24—Radiographs of forelimb elements of *Ancalecetus simonsi*, CGM 42290 (holotype). A, right scapula (Sc). B, left humerus, radius, and ulna (H, R, U). All about 1/3 natural size. Note the fused elbow joint in B, and the absence of any evident pathology in these elements.

Cuneiform.—The cuneiform (Cun in Fig. 22) is the most dorsal carpal in the proximal row. It articulates proximally with the ulna, dorsally with the pisiform, distally with the unciform, and ventrally or radially with the lunar. The cuneiform is fused to all of the elements it contacts except the unciform. The articular surface with the ulna is rather irregular, and fusion is more pronounced in some areas than in others.

The cuneiform measures about 15.1 mm proximodistally, 32.4 mm dorsoventrally, and 13.6 mm mesiolaterally.

Unciform.—The unciform (Unc in Fig. 22) is the most dorsal carpal in the distal row. It articulates proximally with the cuneiform and lunar, and ventrally with the magnum part of the magnum-trapezoid. The unciform is free from the cuneiform, but fused to the lunar and magnum-trapezoid. The unciform has distal articular surfaces for metacarpals V, IV, and part of III (the metacarpals themselves are not preserved). These metacarpal surfaces are smaller and more irregular around their edges than homologous surfaces in *Dorudon*. The unciform was not fused to any of the metacarpals.

The unciform measures about 19.0 mm proximodistally, 24.6 mm dorsoventrally, and 17.0 mm mesiolaterally.

Magnum-Trapezoid.—The magnum and trapezoid (Mag and Trd in Fig. 22) in *Ancalecetus* are joined as a single bone, probably as a result of co-ossification early in normal development. Fusion of the magnum-trapezoid is also found in *Basilosaurus isis* (Gingerich and Smith, 1990) and *Dorudon atrox* (Uhen, 1994, 1996). This composite bone is the central element in the distal carpal row. The magnum part of the composite is dorsal and larger, contacts the unciform, lunar, and scaphoid (the first two contacts are fused contacts, while the latter carpal

FIG. 25—Radiograph of right forearm and carpus of *Ancalecetus simonsi*, CGM 42290 (holotype), shown natural size. Abbreviations from Table 1 are: **Cun**, cuneiform; **Lun**, lunar; **Mag**, magnum; **Pis**, pisiform; **R**, radius; **Trd**, trapezoid; **U**, ulna; **Unc**, unciform. Note carpal fusion (compare forearm of *Dorudon atrox* in Fig. 26 on facing page), and absence of any evident pathology that might explain this.

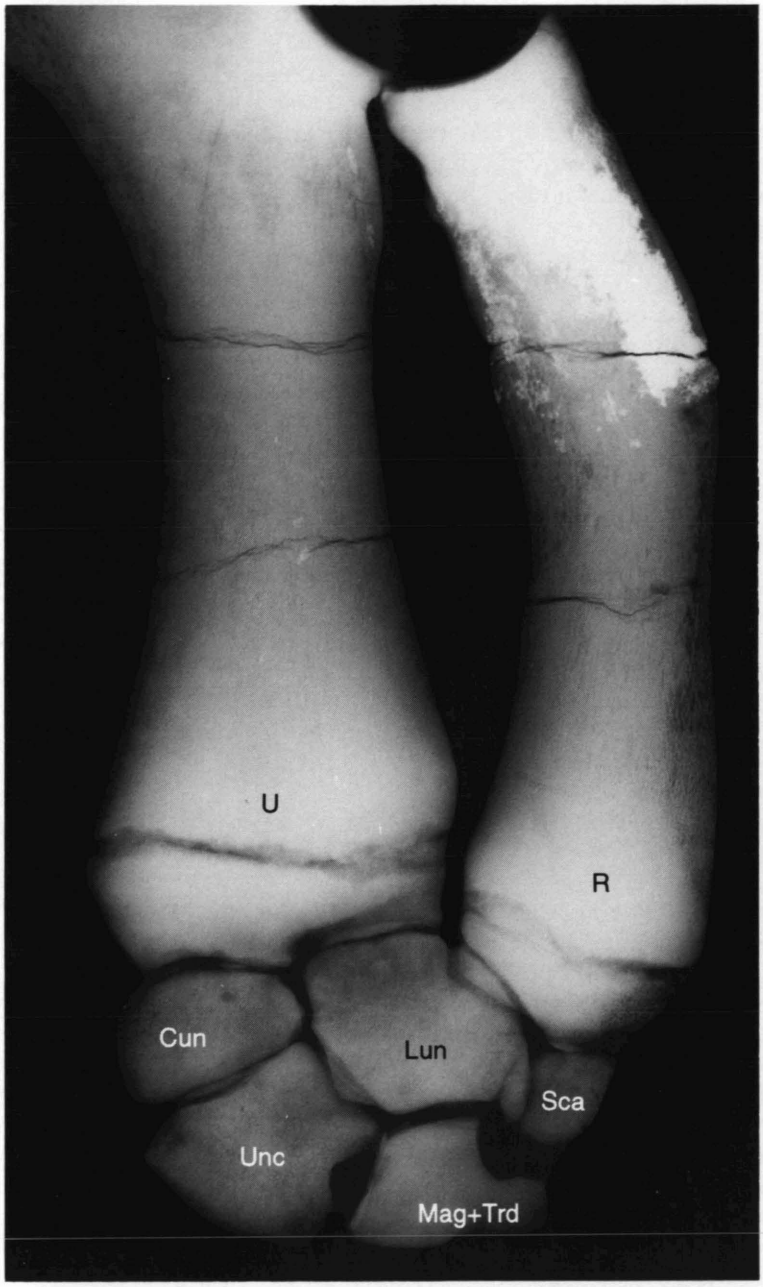

FIG. 26—Radiograph of right forelimb and carpus of *Dorudon atrox*, UM 100222, shown natural size. Abbreviations from Table 1 are: **Cun**, cuneiform; **Lun**, lunar; **Mag**, magnum; **R**, radius; **Sca**, scaphoid; **Trd**, trapezoid; **U**, ulna; **Unc**, unciform. Note the lack of fusion of carpals and lack of fusion of distal epiphyses (compare with unusual forelimb of *Ancalecetus simonsi* in Fig. 25 on facing page).

is not preserved and this contact was evidently unfused), and has a distal facet for articulation of a small metacarpal III (metacarpal III is not preserved). The trapezoid part of the composite is more ventral and smaller. Contacts with the scaphoid and trapezium are indicated by irregular textured surfaces, but neither of these contacting bones are preserved and the contacts cannot have been solidly fused. The trapezoid part of the bone has a distal facet for articulation with a small metacarpal II (see below).

The magnum-trapezoid measures about 14.1 mm proximodistally, 24.0 mm dorsoventrally, and 15.6 mm mesiolaterally.

Trapezium.—The trapezium of *Ancalecetus simonsi* is not preserved in CGM 42290, but there is an irregular textured surface on the ventral side of the trapezoid for articulation with a small trapezium, so a trapezium was clearly present in *Ancalecetus*.

Pisiform.—The pisiform (Pis in Fig. 22) is smaller than the pisiform of other basilosaurids. It is fused to the dorsal surface of the cuneiform and also articulates with the humerus, but the latter contact does not appear to be fused. The pisiform is a relatively flat bone with a distinct distal hook in its dorsal end.

The pisiform measures about 17.0 mm proximodistally, 22.3 mm dorsoventrally, and 9.4 mm mesiolaterally.

Mc II.—The only identifiable hand bone distal to the carpus is a right metacarpal II (Fig. 13K), which fits the metacarpal facet on the distal surface of the trapezoid part of the magnum-trapezoid described above. The bone has a straight body, oval in cross-section, with both proximal and distal articular surfaces damaged. It has the proportions of a metacarpal and was identified by matching remnants of articular surfaces with those on a complete set of metacarpals of *Dorudon atrox*.

Measurements of the second metacarpal are L = 40.1 mm (probably about 44 mm in life); DVW = 13.2 : 9.7 : ca. 12 mm; MLH = 11.3 : 7.4 : --- mm.

DISCUSSION

Our first concern studying CGM 42290 was whether this is an aberrant individual of *Dorudon atrox*, the common basilosaurid of the same size found in the same stratigraphic interval in Wadi Hitan. Such a problem might have been most easily solved by finding more individuals like CGM 42290, but no similar specimens were found. However, collection of some ten good skeletons of *Dorudon atrox* enabled us to characterize its variability (Uhen, 1996), providing the necessary base for comparison of CGM 42290.

CGM 42290, the type specimen of *Ancalecetus simonsi*, is similar in many comparable aspects to *Dorudon atrox*, however it differs significantly in two. The malleus of the ossicular chain transmitting sound to the inner ear is somewhat different in proportions from that of *D. atrox* and it is substantially different in orientation (Fig. 8). The functional significance of these differences has not been studied, but some functional distinction is implied. Secondly, and most obviously, the forelimb of *A. simonsi* is reduced in size and different from *D. atrox* and other basilosaurids in having a relatively narrow scapula (Fig. 23), very limited motion at the shoulder joint, solid fusion at the elbow (Fig. 24), and considerable fusion of wrist elements (Figs. 25-26). Taken together, these mean that the forelimbs of *A. simonsi* were habitually and necessarily carried extending posteriorly and positioned flat against the rib cage as shown in Figure 27A. Functionally, this means that they cannot have been used as anterior horizontal stabilizing fins or flippers controlling dorsoventral movement of the head and thorax, nor could they have been used for turning or other complex maneuvers typical of active cetacean swimmers.

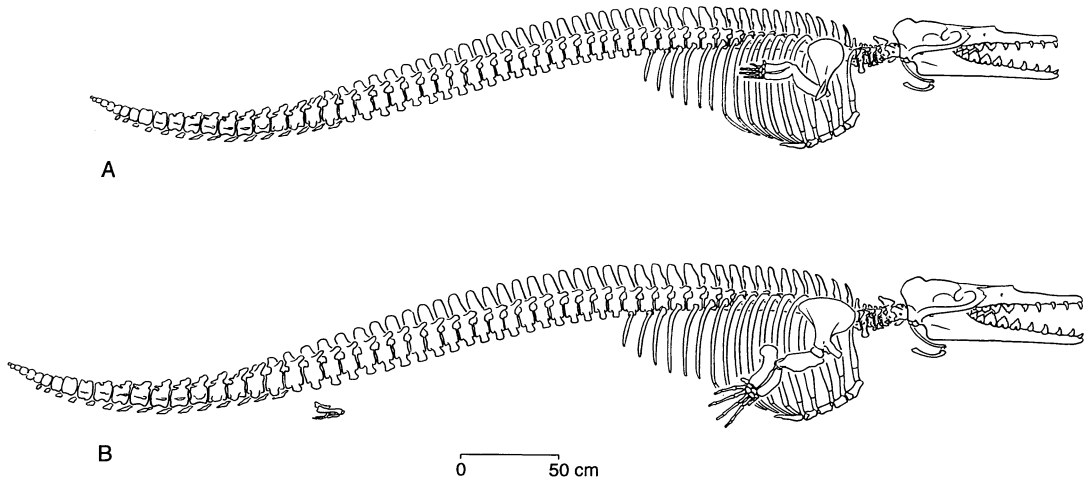

FIG. 27—Reconstruction of *Ancalecetus simonsi* compared to that of *Dorudon atrox*. A, reconstruction of *A. simonsi* based on CGM 42290 (holotype) described here. B, reconstruction of *D. atrox* based on CGM 42183 and UM 97512, 100146, 101215, and 101222 (Uhen, 1996). Both skeletons are drawn to the same scale, but the length of the *A. simonsi* skeleton is speculative, based on elements shown in Fig. 3 in comparison to similar elements of *D. atrox*. Note distinctly different forelimbs of these two contemporary dorudontine archaeocetes.

An advanced archaeocete with such limited swimming capability seems dysfunctional by comparison with active swimmers like contemporary *Dorudon atrox* (Fig. 27B), but well developed masticatory wear on teeth, and fusion of skull bones and epiphyses on vertebrae show that the one known individual of *Ancalecetus simonsi* lived to adulthood. The forms of left and right forelimb elements in *A. simonsi*, to the extent that they can be compared (notably the scapulae and humeri), are perfectly symmetrical bilaterally, which rules out modification due to injury during life. Radiographs show no evidence of the bone remodelling one would expect to be associated with injury. There is no evidence of pathological bone growth in the surface textures of bones, nor again do radiographs suggest pathology. It is possible that the unusual forelimbs of *A. simonsi* represent a rare developmental anomaly, which could explain its symmetry on both left and right sides, but so rare an anomalous individual would not be expected to live to adulthood as evidenced by tooth wear and the cranial and epiphyseal fusions just mentioned. We conclude that CGM 42290 represents a viable evolutionary experiment in cetacean morphology, albeit one that probably did not give rise to any subsequent diversity of whales.

From a functional point of view, it is difficult to comprehend how a basilosaurid like *Ancalecetus simonsi* could be an active swimmer without more mobile forelimbs for stabilization and guidance. The vertebrae that are known, admittedly only 20 compared to the 65 of *Dorudon atrox*, compare well to those of *D. atrox*, suggesting that it may have been an active swimmer. We have reconstructed *Ancalecetus* as having had the long and heavy tail of an active caudally-powered cetacean. However, the lengths of the body and tail are speculative and will remain so until a more complete vertebral column of *Ancalecetus* is found.

Ancalecetus simonsi increases the number of genera and species of latest Bartonian to earliest Priabonian archaeocetes known from the Gehannam and Birket Qarun formations of Wadi Hitan. These are, from largest to smallest:

Basilosaurus isis (Andrews, 1904)
Pontogeneus? brachyspondylus (Müller, 1849)
Dorudontine with intermediate lumbar centra (possibly two taxa)
Dorudon atrox (Andrews, 1906)
Ancalecetus simonsi, new genus and species

Basilosaurus isis and *Dorudon atrox* are both very common in Wadi Hitan. These are represented by many more or less complete skeletons that include evidence of greatly reduced but still functional hind limbs (Gingerich et al., 1990; Uhen, 1996). *Pontogeneus? brachyspondylus* is represented by one association of two large lumbar vertebrae. The dorudontine with intermediate lumbar centra is known from several poorly-preserved partial skeletons in the Cairo Geological Museum and University of Michigan collections. Two taxa of the latter may be represented, but known specimens are inadequate to permit a clear determination. *Ancalecetus simonsi* is known only from the one well-preserved partial skeleton described here. *B. isis*, *P.? brachyspondylus*, and *D. atrox* are all known from the Birket Qarun Formation in and north of Birket Qarun in Fayum (the source of many specimens in the museums of Cairo, Berlin, Frankfurt, London, and Stuttgart). Another basilosaurid, *Saghacetus osiris*, is common in the upper Qasr el-Sagha Formation north of Birket Qarun but it has never been found in the Gehannam or Birket Qarun formations north of Birket Qarun nor has it been found in Wadi Hitan.

Ancalecetus is clearly an advanced archaeocete like other basilosaurids. It differs in many ways from protocetids. Within Basilosauridae, *Ancalecetus* has the vertebral proportions of a dorudontine rather than a basilosaurine. Here we have compared *Ancalecetus* almost exclusively to *Dorudon* because *Dorudon* is both similar in many ways and common in the Birket Qarun Formation where *Ancalecetus* is found. *Ancalecetus* has reduced carpal elements the size of those of North American *Zygorhiza*, but it has the derived developmental fusion of the magnum-trapezoid that unites *Dorudon* with *Basilosaurus*, which may be an important difference from *Zygorhiza* (Kellogg, 1936, fig. 74). We interpret the small size of the carpals of *Ancalecetus* relative to the rest of the skeleton as reflecting the general reduction seen in other forelimb elements.

ACKNOWLEDGMENTS

We thank Mohammed el-Bedawi, Director, and Yusry Attia, Curator, Cairo Geological Museum, for permission to study the type specimen of *Ancalecetus simonsi* at the University of Michigan. Elwyn L. Simons and Prithijit Chatrath of Duke University facilitated field work in Wadi Hitan. Prof. Michael DiPietro provided the radiographs. Alex van Nievelt and William J. Sanders prepared CGM 42290. Bonnie Miljour drew Figures 3, 5, 8, and 27 and helped with preparation of all illustrations for publication. Field research was funded by grants 3424-86, 4154-89, 4624-91, and 5072-93 from the National Geographic Society to P.D.G. and E.L.S., and field work was carried out in cooperation with a long-term Duke University field project in Egypt funded by the National Science Foundation.

LITERATURE CITED

ANDREWS, C. W. 1906. A descriptive catalogue of the Tertiary Vertebrata of the Fayum, Egypt. British Museum (Natural History), London, 324 pp.

BARNES, L. G. and E. D. MITCHELL. 1978. Cetacea. *In*: Evolution of African Mammals, V. J. Maglio and H. B. S. Cooke (eds.), Harvard University Press, Cambridge, 582-602.

BUFFRÉNIL, V. d., A. d. RICQLÈS, C. E. RAY, and D. P. DOMNING. 1990. Bone histology of the ribs of the archaeocetes (Mammalia: Cetacea). Journal of Vertebrate Paleontology, 10: 455-466.

DOMNING, D. P., G. S. MORGAN, and C. E. RAY. 1982. North American Eocene sea cows (Mammalia: Sirenia). Smithsonian Contributions to Paleobiology, 52: 1-69.

FLOWER, W. H. 1885. An Introduction to the Osteology of the Mammalia, Third Edition. MacMillan and Co., London, 382 pp.

FRAAS, E. 1904. Neue Zeuglodonten aus dem unteren Mitteleocän vom Mokattam bei Cairo. Geologische und Paläontologische Abhandlungen, Jena, Neue Folge, 6: 197-220.

GINGERICH, P. D. 1992. Marine mammals (Cetacea and Sirenia) from the Eocene of Gebel Mokattam and Fayum, Egypt: stratigraphy, age, and paleoenvironments. University of Michigan Papers on Paleontology, 30: 1-84.

——— and B. H. SMITH. 1990. Forelimb and hand of *Basilosaurus isis* (Mammalia, Cetacea) from the middle Eocene of Egypt (abstract). Journal of Vertebrate Paleontology, 10A: 24.

———, B. H. SMITH, and E. L. SIMONS. 1990. Hind limbs of Eocene *Basilosaurus isis*: evidence of feet in whales. Science, 249: 154-157.

LANCASTER, W. C. 1990. The middle ear of the Archaeoceti. Journal of Vertebrate Paleontology, 10: 117-127.

MILLER, M. E., G. C. CHRISTENSEN, and H. E. EVANS. 1964. Anatomy of the Dog. W. B. Saunders Co., Philadelphia, 941 pp.

NORRIS, K. S. 1980. Peripheral sound processing in odontocetes. *In*: Animal Sonar Systems, R.-G. Bushnel and J. F. Fish (eds.), Plenum Publishing Co., 495-509.

OSBORN, H. F. 1907. Hunting the ancestral elephant in the Fayum desert. Century Magazine, 74: 815-835.

POMPECKJ, J. F. 1922. Das Ohrskelett von *Zeuglodon*. Senckenbergiana, Frankfurt, 4: 44-102.

ROMMEL, S. 1990. Osteology of the bottlenose dolphin. *In*: The Bottlenose Dolphin, S. Leatherwood and R. R. Reeves (eds.), Academic Press, San Diego, 29-49.

STROMER, E. 1903. *Zeuglodon*-Reste aus dem oberen Mitteleocän des Fajum. Beiträge zur Paläontologie und Geologie Österreich-Ungarns und des Orients, Vienna, 15: 65-100.

———. 1908. Die Archaeoceti des ägyptischen Eozäns. Beiträge zur Paläontologie und Geologie Österreich-Ungarns und des Orients, Vienna, 21: 106-178.

UHEN, M. D. 1994. Forelimb of late middle Eocene *Prozeuglodon atrox* (Mammalia, Cetacea) from Fayum, Egypt (abstract). Journal of Vertebrate Paleontology, 14A: 50.

———. 1996. *Dorudon atrox* (Mammalia, Cetacea): form, function, and phylogenetic relationships of an archaeocete from the late middle Eocene of Egypt. Ph.D. dissertation, University of Michigan, 608 pp.